Journal of Material Cycles and Waste Management (2023) 25:1988–2011
https://doi.org/10.1007/s10163-023-01713-9

REVIEW

Synthesis of artificial aggregates and their impact on performance of concrete: a review

Gopal Bharamappa Bekkeri[1] · Kiran K. Shetty[1] · Gopinatha Nayak[1]

Received: 6 October 2022 / Accepted: 16 May 2023 / Published online: 27 May 2023

Abstract

Infrastructure development and urbanization have created a demand for the prime construction material—"Concrete." The manufacture of concrete has pressurized the aggregate supply chain for over-exploitation of natural resources leading to eco-detrimental impacts besides environmental regulations. The auxiliary sectors of the construction industry are creating a vast quantum of by-products and waste, causing environmental degradation, which concerns governing bodies. Developing aggregates artificially using these by-products and waste materials would be an eco-friendly and economical solution. This article provides an overview of the ingredients, production methods, and factors influencing the characteristics of such sustainable building materials, which can substitute conventional aggregates in the near future.

Keywords Artificial aggregates · Lightweight aggregates · Lightweight aggregate concrete · Pelletization · Fly ash

Introduction

Population explosion, elevated economy, lifestyle, and urbanization require the consumption of natural resources at large, thereby creating scarcity. The need for secured shelter for humankind and infrastructure competence has escalated the phase of construction activities. This demand has created a shortage of raw materials for concrete production. Natural resources are being over-exploited, hence an increasing concern over long-term sustainability [1, 2]. It is well known that aggregates occupy a significant volume of concrete, and approximately two tons of aggregates are essential to manufacture one cubic meter of concrete. The global demand for aggregates was about 51.7 billion metric tons in the year 2018, which was expected to escalate at a rate of 5.2% annually [3]. Sustainable construction is captivating the attention of researchers worldwide to conserve the environment and natural resources. On the flip side of the construction sector, the auxiliary industries are generating waste on a large scale. The waste includes materials like ashes, slag, sludge, etc. In the industrial and construction sectors, reduce, reuse and recycle are the basic principles to attain economic and sustainable values. The inherent characteristics of industrial and construction wastes show their fitness for utilization as building materials. However, some waste materials are unsuitable for direct use without prior treatment because of their eco-detrimental properties [4]. With minimal processing, many such by-products can replace conventional raw materials.

One of the approaches to utilize various wastes in large quantities is to produce aggregates artificially by pelletization (also known as agglomeration). These find their practical application in producing lightweight concrete. Artificial aggregates are produced by allowing powder materials to agglomerate to form ball-like rounded pellets by sprinkling the optimum quantum of liquid in the pelletizer. During pelletization, wet particles bind together with cohesive and tumbling forces. Thus, the pelletization technique attracts researchers as they can reduce the demand for natural aggregates. The aggregates in a fresh state might lack sufficient strength; hence, hardening methods like cold-bonding or sintering are carried out [5]. It is also possible to manufacture artificial aggregates through pressing, expansion (bloating), and crushing. However, producing artificial aggregates using the pelletization process is regarded as a well-developed agglomeration technique. The production and characteristics of the artificial aggregates mainly depend on the methodology and properties of raw materials, type of binder, size,

✉ Kiran K. Shetty
kiran.shetty@manipal.edu

[1] Department of Civil Engineering, Manipal Institute of Technology, Manipal Academy of Higher Education, Manipal 576104, Karnataka, India

specific surface area, and the wettability of the particles. Nevertheless, the composition and dosage of binder in the production process significantly impact the engineering properties of the produced aggregates [6].

The construction industry is a welcoming receptor of different industrial, municipal, and agricultural wastes as it can digest vast quantities of waste by galloping them in the composites. Concrete is an extensively used and globally well-accepted construction material because of its mechanical properties and durability. However, the self-weight of concrete structures accounts for a large amount of design loads, substantially impacting the construction project cost. The coarse aggregate claims the prime share of the weight of concrete, which can be subsided by adopting lightweight aggregates. The usage of pelletized aggregates (artificial aggregates) in concrete production makes it lightweight with reduced dead load, resulting in the reduced dimension of the structural elements and reinforcement quantity. Further, it provides better thermal comfort, improved sound insulation, increased resistance against earthquake forces, reduced labor requirements, low transportation costs, and less machinery effort needed for concrete handling. Lightweight aggregate concrete is a significant and adaptable material in current construction activities and is used in constructing offshore structures, long-span bridges, high-rise buildings, and precast components [7–9].

The artificial lightweight aggregates are cost effective as these are manufactured by employing waste materials. Waste materials such as ash, sludge, and slag are the most suitable options for producing lightweight aggregates. The fractional replacement of cement (OPC) and sintering at high temperatures is essential to producing robust and durable aggregates [10]. It has gained interest and huge industrial demand due to its unique properties and significant economic and environmental benefits. These are produced artificially by sintering or cold-bonding, in which the sintering method requires a high temperature of around 1000–1200 °C to produce solid and lightweight aggregates by consuming ample energy and emitting considerable carbon dioxide (CO_2) gas. On the contrary, the cold-bonding technique requires less than 100 °C temperature to produce aggregates, and it consumes little energy with zero emission of CO_2. Therefore, cold-bonded aggregates have sustainable value globally due to their cost-effective processing methods and environmental aspects [11]. For additional carbon footprints, artificial aggregates are produced by pelletizing the industrial wastes using alkali activators with promising results in physio-mechanical properties and durability [12]. The cost of making artificial aggregates is higher than that of producing natural aggregates as it requires unique machinery and trained human resources [6]. In addition, artificial aggregates containing cement emit CO_2 during manufacturing and increase aggregates' production costs [10].

This article seeks to review existing information about the production of artificial aggregates with both cold-bonded and sintering techniques and their applications in concrete production. This review paper is outlined as follows; (1) types of raw materials and binders and their impact on the properties of aggregates; (2) manufacturing process of artificial aggregates; (3) factors affecting the manufacturing process and characteristics of aggregates; (4) microstructure and mechanical properties of artificial aggregates; and (5) fresh, physical, mechanical, and durability properties concrete incorporated with artificial aggregates.

Types of artificial aggregates covered

This review mainly covers two types of artificial aggregates (AA): cold-bonded artificial aggregates (CB-AA) and sintered artificial aggregates (ST-AA). Both types can be differentiated only by the hardening method. The CB-AA are hardened after fresh production by employing a temperature of less than 100 °C, whereas ST-AA at high temperatures over 1000 °C to fuse the particles. Based on the raw materials used for the production, the CB-AA have been categorized into cold-bonded cementitious-based artificial aggregates (CB-CM-AA) and cold-bonded alkali-activated artificial aggregates (CB-AAA). The detailed production process and hardening method of all artificial aggregates are discussed in the succeeding sections.

Raw materials

Table 1 lists various raw materials, binders, and special additives used for the manufacture of cementitious, sintered, and alkali-activated artificial aggregates. Fly ash (FA) is the main basic ingredient for manufacturing all types of aggregates because of its low cost, abundance, and global availability. However, it will be eco-detrimental if it is unattended in a short span. Along with FA, other wastes used are listed as sewage sludge (SS), washing aggregate sludge (WAS), marble sludge (MS), wastewater treatment sludge (WTS), desulfurization device sludge (DDS), peat-wood fly ash (P), municipal solid waste incinerator bottom ash (MSWI-BA), municipal solid waste incinerator fly ash (MSWI-FA), paper sludge ash (PSA), pond ash (PA), rice husk ash (RHA), bottom ash (BA), bottom ash fines (BAF), weathered fly ash (WFA), incinerated sewage sludge ash (ISSA), quarry dust (QD), cement kiln dust (CKD), river sediment (RS), and red mud (RM).

During the manufacturing of cementitious-based artificial aggregates, it is essential to integrate the binders when the raw materials contain poor cementitious properties. As listed in Table 1, binders such as cement (OPC),

Table 1 Raw materials, binders, and additives used to produce artificial aggregates

Type of AA	Precursors and Binders	Activators and [Additives]	Angle/Speed/Duration	Curing regime	References
CB-AAA	FA (class-F)	NaOH and Na_2SiO_3	45°, 40 rpm, 15 min	Ambient, heat, solution and heat-solution	[3]
CB-AAA	FA (class-F)	NaOH and Na_2SiO_3	35°–55°, 30–50 rpm, 12–18 min	Ambient, heat and solution	[6]
ST-AA	RM, MSWI-BA	Water	15 min	Room temp. for 24 h then sintered at 400 °C–1000 °C	[1]
CB-AAA	RM, FA (class-C)	Na_2SiO_3	40°, 55 rpm, 15 min	22 °C and 50% relative humidity (RH)	[35]
CB-CM-AA	FA (class-F), GGBS, OPC	Na_2SiO_3, water	Crushing technique	Oven curing at 105 °C–24 h then room temp. (sealed in plastic bags)	[16]
CB-AAA	FA (class-F)	NaOH and Na_2SiO_3	48°, 60 rpm, 20 min	Room temp. at 20 °C and 95 ± 5% RH	[36]
CB-CM-AA CB-AAA	FA (class-F), GBFS, OPC	NaOH and Na_2SiO_3		Room temp. at 20 °C , water curing for CB-CM-AA, Oven curing 70 °C–24 h for CB-AAA	[2]
CB-AAA	FA (class-F), MSWI, LM	NaOH and Na_2SiO_3	48°, 60 rpm, 20 min	Room temp. at 20 °C–24 h and 95 ± 5% RH	[37]
CB-AAA	FA (class-F)	NaOH and Na_2SiO_3	45°, 50°, 55°, 26 rpm	Room temp	[38]
CB-CM-AA	BA, OPC	Water	50°–60°, 45–55 rpm	Room temp. at 21 °C , and 94% RH	[39]
ST-AA	MSWI-BA, RHA	Water		Oven curing at 105 °C then sintered at 1100 °C	[30]
CB-AAA	FA (class-F)	NaOH and Na_2SiO_3	Crushing method	Room temp. at 20 °C and 40–60% RH	[16]
ST-AA	MSWI-FA, MSWI-BA, RS	Water	Hand shaping	Oven curing at 105 °C then sintered at 950 °C–1150 °C	[40]
CB-AAA	FA (class-F)	NaOH and Na_2SiO_3	45°, 40 rpm, 15 min	Room temp. at 28 ± 2 °C and 80% RH then heat curing at 60 °C and 80 °C	[41]
ST-AA	SS, RS	Water	Hand shaping	Drying at 110 °C then sintered at 900 °C–1200 °C	[42]
CB-AAA	FA (class-F)	NaOH and Na_2SiO_3	45°, 10 rpm, 15 min	Room temp. at 28 ± 2 °C and 80% RH, then heat curing at 80 °C , SC	[31]
CB-CM-AA	EP, EPP, FA (class-F), OPC	Water	35°–45°, 20–30–40 rpm, 15 min	Room temp. at 21 ± 1 °C	[11]
CB-CM-AA	OPC, FA (class-F), PPA, WAS, BAF, GGBS	Water		Sealed in buckets at room temp	[4]
CB-AAA	P, FA (class-C), GGBS, MK	K_2SiO_3, $NaAlO_2$, water, KOH, NaOH	33°, 44 rpm	Room temp. and sealed in bags	[10]
CB-CM-AA	OPC, FA (class-F), QD	Water	25°, 26 rpm	Water curing	[26]
CB-CM-AA	MSWI-FA, lime, OPC, FA	Water	45°, 45 rpm	climatic chamber curing at 50 °C and 95% RH	[12]
ST-AA	FA (class-F), BT	NaOH	36°, 55 rpm, 15 min	Oven curing at 100 °C then sintered at 950°	[25]
ST-AA	LM	NaOH and Na_2SiO_3	Hand mixer	Sintered at 950 °C	[43]
ST-AA	FA (class-F)	Water	40°, 35 rpm	Room temp.at 27 °C and 70% RH, then sintered at 950 °C	[24]
CB-CM-AA	FA (class-F), GGBS, BT, MK	NaOH	36°,55 rpm,10–15 min	Oven curing at 100 °C –7 days	[44]

Table 1 (continued)

Type of AA	Precursors and Binders	Activators and [Additives]	Angle/Speed/Duration	Curing regime	References
CB-CM-AA	Pond ash, OPC, lime	Water, $[Ca(OH)_2]$, Na_2SO_4	14-7 min	Water curing	[5]
CB-CM-AA	FA (class-F), GGBS, BT, MK	NaOH	36°, 55 rpm	Oven curing at 100 °C	[33]
ST-AA	Pond ash, clay, kaolin, BT	$[Ca(OH)_2]$, Water	50°, 50 rpm	Oven curing at 105 °C then sintered at 900 °C–1100 °C	[21]
CB-CM-AA	FA (class-F), OPC, GGBS, BT, MK	NaOH	36°, 55 rpm	Oven curing at 100 °C–7 days	[44]
CB-CM-AA	CKD, GBFS, MS	Water	50°, 35–45-55 rpm	Room temp. at 100% RH-56 days	[45]
ST-AA	OPC, FA (class-F), SS, GP	Water glass	Granulator	Oven curing at 105 °C then sintered at 830 °C–1100 °C)	[46]
CB-AAA	Pulverized bottom ash	$[Ca(OH)_2]$, NaOH, Na_2SiO_3		Ambient curing at 30° and 32°	[34]
CB-CM-AA	WFA, WTS, DDS	Water	55°, 45 rpm	Room temp. at 100% humidity-56 days then thermal curing at 40 °C	[47]
CB-CM-AA	FA (class-F), GGBS, RHA, OPC	NaOH and Na_2SiO_3	53°, 35 rpm	Room temp. at 23 °C and 60% RH	[22]
CB-CM-AA	OPC, slag, FA (class-F)	Water	45°, 45 rpm, 20 min	Room temp. at 21 °C and 71% RH	[48]
CB-AAA	FA (class-F), OPC, lime	NaOH	36°–55°	Oven curing at 100 °C–7 days	[32]
CB-CM-AA	MSWI-BA, OPC, lime, FA	Water	55 rpm	Thermal curing at 40 °C and 95% RH-28 days	[49]
ST-AA	FA (class-F), BT, GP	Water	43°,45 rpm, 20 min	Oven curing at 110 °C then sintered at 1100 °C —1200 °C	[29]
ST-AA	OPC, FA (class-F), BT, GP, SF	Water	43°, 45 rpm	Oven curing at 110 °C then sintered at 1100 °C —1200 °C	[50]
ST-AA	WAS, FA (class-F), used motor oil	Water	Hand shaping	Oven curing at 105 °C–48 h, then sintered at 1150 °C –1225 °C	[51]
–	FA (class-C)	Water	55°, 55 rpm	Water curing at 24 °C , autoclaving at1mpa pressure-2 h, steam curing at 70 °C–90 min	[52]
CB-CM-AA	OPC, FA (class-C)	Water	43°, 35 rpm	Room temp. at 20 °C and 70% RH	[27]
ST-AA	FA (class-F)	Water	20°–40°, 40–70 rpm	Sintered at 1100 °C–1 h	[15]
ST-AA	FA (class-F and -C)	Water	55°, 40 rpm	Sintered at 1100 °C–1 h	[53]

lime, bentonite (BT), metakaolin (MK), and glass powder (GP), have been used to agglomerate the raw materials for pelletization. Cement is proved to be the best binder material for this purpose; however, studies are being executed to reduce or nullify the use of cement, as its production process is eco-detrimental. To subside cement usage, mineral admixtures can be effectively replaced, and geopolymers are promising alternatives with a minimal carbon footprint. In producing alkali-activated or geopolymer-based aggregates, alkaline activators prepared using silicates and hydroxides of either sodium, potassium, or calcium are used. Along with these, sodium sulfate (Na_2SO_4), expanded perlite powder (EPP), and reactive silica (SF) are also adopted as special additives during the production of artificial aggregates.

Manufacturing process

Basic methods for producing fresh aggregates

Four manufacturing methods can be employed to manufacture artificial aggregates and are outlined as follows.

Pelletization

It is a method of effective agglomeration which transforms finer moisturized particles into larger-sized solid material. The formed pellet material attains strength through their collision caused by the rolling movement in the pelletizer disc. Pelletizer requires minimal operation space, and the pellets' size can be controlled with less effort when compared to drum or cone pelletizers [13–15]. The performance of pelletization is influenced by the factors like moisture content, specific surface area, wettability, size, and shape of particles. It is also governed by the speed and angle of the pelletizer, as well as the duration of the pelletization process [13, 15]. At low speeds, the movement of the pellets is influenced by gravitational force, and at high speeds, it is influenced by centrifugal force. If one of these factors occurs, either the pellet formed has a loose structure or the formation is ceased [15]. The proper collision between the moisturized fine particles is ensured by properly adjusting the disc's angle and speed, which increases production efficiency [14].

Crushing method

It is the method of crushing the hardened paste into small fractions of the required size by hammering action and curing the crushed particles until the testing period. The crushing method enables the production of artificial aggregates of angular size, which is more suitable for mass production than the pelletization method. Xu et al. reported a detailed procedure to produce aggregates by crushing [16].

Mould casting

The required shape and size aggregates are obtained by casting the paste in the moulds, followed by curing in closed conditions until the testing period. The commonly employed procedure is casting reactive foam mixture into a spherical shape with the help of a polystyrene mould or into an aggregates shape using a plastic pipette [17, 18].

Hand shaping

The aggregates are produced manually by hand, which is unsuitable for mass production [16, 17].

Pellet formation and growth mechanism

The nucleation, transition, and ball development zones are the three sequential regions that make up the most compelling classification of the pelletization process. This process was suggested based on experiments on the mechanism of pellet creation and growth. When a powder is moisturized with a solvent system, the pelletization process enters the nucleation stage. Three-phase nuclei systems comprised of air, water, and liquid are created from the primordial particles and kept together by liquid bridges with pendular shapes, as shown in Fig. 1. Their bonding strength will enhance as the particle size is reduced. The size of the particles, moisture content, the binding particles' viscosity, the substrate's wettability, and processing parameters, such

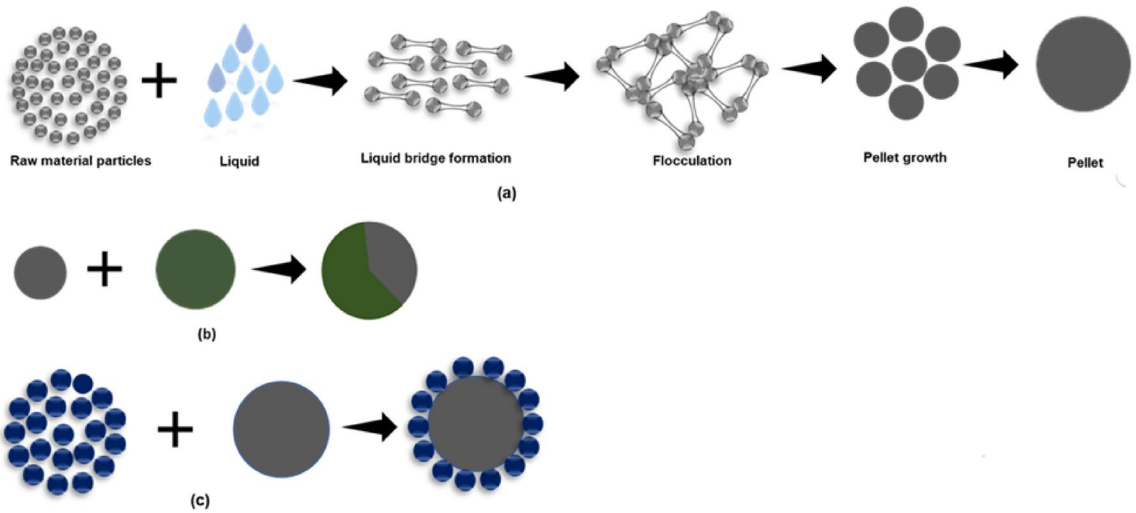

Fig. 1 Schematic diagram of pellet formation and growth mechanism **a** Nucleation **b** Coalescence, and **c** Layering

as tumbling and drying rates, will affect the size, rate, and degree of nuclei production. Nucleation is succeeded by a transition period where coalescence and layering are the dominant growth mechanisms. The nucleation, coalescence, and layering process are depicted in Fig. 1.

Coalescence is the formation of large-sized particles by the chance of collision of well-formed nuclei, which necessitates a slight excess of moisture on the nuclei's surface. Through this process, the number of nuclei gradually decreases; however, the system's overall mass stays constant. Layering is a gradual development method that builds existing nuclei with successive additions of fines and fragments. In this step, the system's overall mass matures due to the rising particle size as a function of time while the number of particles stays constant [19, 20].

Pelletization Process

The artificial aggregates preparation process uses pelletizer equipment with a diameter of about 500 mm–1200 mm, tilting ability between 0° and 90°, and speed variation of 5 rpm to 60 rpm, as shown in Fig. 2. The overall pelletization process includes mixing, granulating, and curing, as shown in Fig. 3. To ensure consistent and proper mixing, the binder and other raw materials are mixed dry for 2–3 min. Then, 75 per cent of the water or activating solution is added to start the agglomeration process. The remaining water is sprayed into the mixture during the pelletization process using an electric spray cannon or sprinkler. The sprayed solution served as a coagulant and wetting agent, causing the wet mixture to roll and get pelletized due to capillary attraction caused by the tilted rotary motion of the pelletizer [21]. Keen monitoring is essential during the sprinkling of solution/water to avoid the formation of slurry muddy balls. In the process of granulation, binding forces include (i) the surface tension and interaction force of the liquid, (ii) electric charge attraction and the Van Der Waals force between powders, (iii) the adhesion of the electric double layer, and (iv) binder viscosity/adhesion [22]. The production of artificial aggregates from the same source of material and granulator type is governed by (i) the angle of the granulator, (ii) the speed of the granulator, (iii) the amount of added admixtures, (iv) the duration of granulation, and (v) the

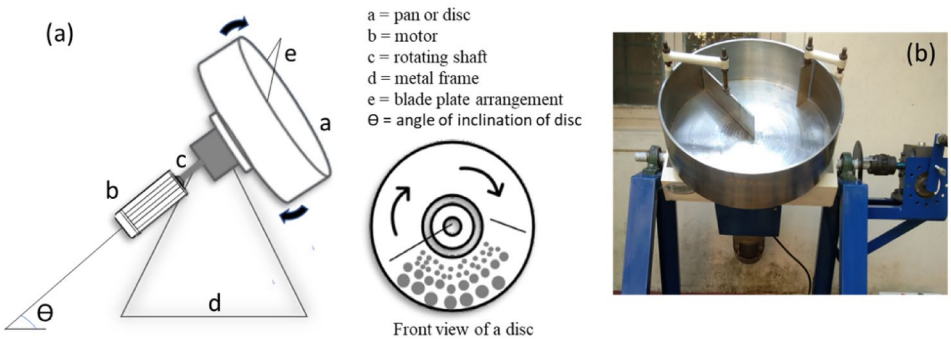

Fig. 2 **a** Schematic view of disc pelletizer **b** Laboratory disc pelletizer

Fig. 3 Pelletization process

quantity of catalyst and binder [15]. The formation of pellets usually occurs between 10 and 15 min, and the total granulation time is determined as 20 min for the formation of fresh pellets. The aggregate pellets in a fresh state shall be handled with care while discharging from the pelletizer and placed at ambient conditions for one day to gain the initial strength, followed by curing for sufficient days [4, 15, 21–28].

Influencing factors on the production process and properties of aggregates

Table 1 shows that the researchers produced different artificial aggregates using various raw materials, binders, and special additives. Additionally, they employed varied pelletizer speeds and angles, different pelletization duration, and curing regimes. The following section reviews the influence of these variables on the characteristics of produced aggregates.

Water content and pelletization efficiency

A moisture content of 15%–35% is suitable for producing fly ash-based pellets, and moisture content beyond that might result in muddy balls [15]. Most research works have adopted water content of between 20 and 30% based on raw material properties [25, 27, 29, 30].

The pelletization efficiency of aggregates is expressed in the percentage weight of aggregates having a size greater than 4.75 mm against the total weight of aggregates produced in a pelletizer [31]. It depends upon the characteristics of raw materials, additives, and alkaline activators. Fly ash with a higher fineness (class-C) does not require any binders to achieve the highest pelletization efficiency [13]. In comparison, fly ash with a lesser fineness (class-F) requires binders to achieve it, as the pelletization efficiency increases with the increase in the content of calcium oxide (CaO) in the raw material, either in the form of ground granulated blast-furnace slag (GGBS) or cement [13, 22, 23, 32, 33]. Adding RHA to FA decreases the pelletization efficiency due to the negligible content of CaO [22]. In geopolymers, the concentration of sodium hydroxide (NaOH) plays a vital role in improving pelletization efficiency [34].

Curing regime

Curing acts as a prime factor in deciding the characteristics of artificial aggregates. Based on the raw materials and ingredients, these require different curing mechanisms are reviewed below.

For cementitious-based aggregates

The employment of normal water curing requires a large area within the production zone. Accelerated curing methods reduce the curing duration, by which aggregates can be produced at a faster phase by saving space, but it leads to more energy consumption. Table 1 shows that the aggregates were cured at a temperature of 20 °C with a relative humidity range of 50–100% in most studies. However, an increase in the duration of normal water curing from 7 to 28 days improved strength and reduced water absorption. Besides, an increase in steam curing and autoclaving duration from 5 to 10 h also enhanced aggregate properties [52].

For alkali-activated aggregates

As mentioned in Table 1, ambient curing, heat curing, solution curing, and heat-solution curing were employed in manufacturing alkali-activated artificial aggregates. The solution-cured aggregates exhibited maximum bulk density and specific gravity over other methods due to the formation of a layer over the aggregates' surface, making it impermeable and solid, but it increases production costs [3]. However, the aggregates subjected to heat curing exhibited less specific gravity, high water absorption, high crushing, and impact strength compared to aggregates subjected to ambient curing [41].

For sintered aggregates

Table 1 shows that the aggregates were also subjected to sintering at high temperatures in the range of 900 °C–1250 °C. The strength of aggregates increases with the increase in temperature and decreases beyond 1070 °C due to liquid-phase mass transfer and the formation of macropores. The aggregates hardened between the temperatures 950 °C–1200 °C depicted excellent physical and mechanical properties, and temperatures more than 1200 °C caused the formation of pores with an expansion and bloating in the inner part of aggregates resulting in inferior characteristics. A temperature of 1100 °C is adequate to produce aggregates with minimum water absorption, specific gravity, and maximum strength [29, 40, 42, 50, 51, 54].

Speed and angle of pelletizer

As mentioned in Table 1, the speed and angle of the pelletizer employed to produce artificial aggregates range from 10 to 60 rpm and 20° to 55°, respectively. The pelletization process most significantly depends on the speed and angle of

the pelletizer; hence it is essential to study their influence on the aggregate production process. Tajra et al. reported that the pelletization efficiency enhanced with increased rotation speed due to the formation of a denser cover matrix over the surface of particles. Besides, an increase in rotation speed caused improved crushing strength, water absorption, bulk density, and particle density [11]. The pellet strength is typically affected by the speed followed by an angle, and water absorption is influenced by the speed of the pelletizer [15]. Increasing either the speed and angle or speed and duration of pelletization lengthens the pellet path, which increases tumbling forces, forming compacted aggregates with low water absorption and high strength [21]. The negligible improvement in the crushing strength, impact strength, and water absorption was observed when the angle and speed of the pelletizer were increased from 30° to 50° and 35 to 55 rpm, respectively [6]. The best strength values were obtained at a speed of 45 rpm. An increase in rotation speed increases the collision and consolidation of nuclei (particles) up to a certain limit, beyond which a subsequent stratification of particles is restrained by centrifugal force. It caused the adhesion of particles on the side walls; finally, it hindered the pelletization process [45]. Baykal et al. revealed that the optimum speed of the granulator should be chosen between 35 and 55 rpm and an angle between 35° and 55° to obtain suitable quality aggregates [55]. The maximum pelletization efficiency could be obtained at an optimum angle of 42° and 45 rpm speed [48, 54].

Influence of precursors/binders

Various raw materials to produce artificial aggregates have been listed in Table 1; the most commonly used were FA, OPC, GGBS, MK, and BT. The pelletized aggregates with cement addition showed higher density, less water absorption, and high impact and crushing strength than aggregates produced with GGBS addition. It is attributed to the higher specific gravity of cement than GGBS and the formation of the compact structure due to the formation of CSH gel [2, 11, 54]. Aggregates produced using only FA led to lower strength and higher water absorption than aggregates produced by blending GGBS and OPC separately with FA [2, 22]. It is also noted that the FA of higher fineness and GGBS improved the pelletization process, while FA of lower fineness decreased the pelletization [23, 37, 43–45].

Table 2 lists the oxide composition of various raw materials commonly used in producing cold-bonded alkali-activated aggregates. Based on the reaction products formed during alkali activation and the percentage of oxides, binders are divided into four distinct groups: Ca–Al, Ca–Si–Al, Fe–Si (Al), and Si. Metakaolin and fly ash are the first Ca–Al group's most commonly used raw materials. When reacting with the alkaline solution, they form N–A–S–H gel with the three-dimensional network as the end product. The most frequently used materials in the Ca–Si–Al group are GGBS and fly ash (class-C), which form both C–A–S–H and N–A–S–H [56, 57]. The third group of raw materials contains a maximum percentage of Fe and Al or Si compared to the previous two groups. In this case, partial tetrahedral Fe^{+} substitutes Al^{+} in the octahedral alumino-silicate structure [18, 58]. Si group contains materials like silica fume, glass powder, and rice husk ash. The final product of these materials would be N–A–S–H when rich silica is present in the precursors combined with the alumina-based alkaline solution.

Influence of activators/geopolymerization factors

Table 1 mentions different types of activators used by the researchers; the most commonly used were NaOH and Na_2SiO_3. An increase in the molarity of NaOH increases bulk density, specific gravity, ten percent fine value (TPFV), and pelletization efficiency along with strength at a given alkaline liquid (LA)/ash ratio and Na_2SiO_3/NaOH ratio; in turn, decreasing open porosity and water absorption [33, 34, 43]. Razak R et al. reported that for a high Na_2SiO_3/NaOH ratio, excess Na_2SiO_3 might inhibit water evaporation and structure formation [21, 43]. Besides, the artificial aggregates manufactured at the high molarity of 16 M exhibit efflorescence, large-sized voids, and less compaction due to excess alkali content causing low workability during palletization [43]. It is also reviewed that the water content of 19%–21% increases the pelletization efficiency and influences the particle size of produced aggregates [31]. Increased Na_2O content (4%–6%) and SiO_2/Na_2O ratio (0.3–0.5) in alkaline activators resulted in improved crushing strength, impact strength, and water absorption [6, 31]. The aggregates exhibit the lowest water absorption for the Na_2SiO_3/NaOH ratio, which equals 2.5 compared to ratios of 1.5, 2.0, and 3.0, as micropores and pore enhancement are proportional to the alkaline activator ratio. The alkaline activator ratio also influences the granulation process as the ratio of Na_2SiO_3/NaOH equals 1.5; produced aggregates were not perfectly round due to slow granulation. At a ratio of 2.0, the aggregates produced were more shaped due to the faster polymerization process; at a ratio of 2.5, the aggregates produced were of uniform shape and size with tiny pores. At a ratio of 3.0, the aggregates produced were larger oval shapes due to the speedy granulation process [38]. For the manufacture of pelletized aggregates, an alkaline solution with a minimum of 6 M concentration was suggested as a lower concentration of NaOH will avoid workability issues during the pelletization process. As the NaOH concentration rises, a higher temperature is required to start and accelerate the polymerization reaction [37]. Aggregates produced using K–Si, and KOH were stronger than aggregates produced using $NaAlO_2$ and NaOH [10].

Table 2 Oxide composition of various raw materials

Category	Oxide's precursors	SiO_2	Al_2O_3	CaO	Fe_2O_3	Na_2O	TiO_2	SO_3	K_2O	P_2O_5	MgO	ZnO	CuO	MnO	Refs.
Si-Al[a]	FA (class-F)-1	60.65	28.62	1.70	3.95	1.11	–	1.26	0.11	–	1.84	–	–	–	[6]
	FA (class-F)-2	43.40	26.90	9.14	9.19	3.16	0.91	1.65	1.28	–	3.49	–	–	–	[16]
	MK-1	54.3	38.3	0.39	4.28	0.12	–	0.22	0.5		0.08	–	–	–	[7]
	MK-2	59.5	32.8	0.1	1.4	0.1	1.9	0.0	0.6	0.00	0.1	–	–	–	[10]
	EPP	76.9	11.3	0.9	–	3.6	–	–	3.6	–	0.1	–	–	–	[11]
	WAS	73.31	11.29	1.46	6.0	0.61	–	0.16	1.85	0.07	0.89	0.01	0.00	0.12	[4]
	Pulverized bottom ash	53.68	18.91	1.24	7.7	0.7	–	0.19	–	–	0.48	–	–	–	[34]
	MSWI-BA	52.0	28.0	8.1	5.0	0.5	–	0.5	0.8	–	1.8	–	–	–	[49]
Ca–Si-Al[b]	GGBS	30.19	12.69	40.01	0.60	–	1.40	3.55	0.62	0.00	9.08	–	–	0.27	[4]
	PSA	13.64	8.64	54.94	0.99	–	0.74	0.99	0.46	0.30	2.09	0.08	0.07	0.03	[4]
	MSWI-BAF	39.13	7.60	18.58	12.93	1.02	–	4.33	1.09	0.86	1.93	0.66	0.38	0.17	[4]
	MSWI-BA	5.2	14.5	33.1	7.9	2.2	–	27.9	1.1	1.9	2.8	–	–	–	[86]
	Peat-wood fly ash(P)	44.9	10.7	11.6	20.1	1.5	0.4	2.0	2.1	2.6	3.0	–	–	–	[10]
	BT	47.84	14.85	2.29	9.61	2.88	–		1.45	–	2.20	–	–	–	[44]
	Bitumen Pond ash	57.2	25.7	2.1	6.9	0.58	–	0.83	–	–	0.41	–	–	–	[5]
	Lignite Pond ash	30.15	22.5	23.6	14.7	0.43	–	0.27	0.35		3.4	–	–	–	[5]
	GBFS	35.16	10.76	41.91	1.40	0.11	–	1.92	0.14		7.68	–	–	–	[45]
	FA (class-C)-1	31.62	30.11	17.17	8.94	0.74	–	5.72	0.10		3.71	–	–	0.02	[52]
	FA (class-C)-2	49.10	22.98	13.61	5.41	0.30	–	1.54	1.13		1.44	–	–	–	[27]
Fe-Si (Al)[c]	PFA	55.6	23.0	1.3	13.8	0.5	–	0.1	2.7	0.5	1.0	–	–	–	[86]
Si[d]	SF-1	93.6	1.3	0.5	0.9	0.4	–	0.45	1.52	–	1	–	–	–	[7]
	GP-1	74.0	6.0	9.7	0.3	8.2	0	0.2	0.8	0	0	–	–	–	[46]
	RHA	91.43	0.35	0.98	0.41	0.08	–	1.40	–	0.98	3.54	–	–	–	[22]
	GP-2	70.62	1.38	8.75	0.82	10.85	–	1.85	1.53	–	–	–	–	–	[29]
	SF-2	94.12	0.57	0.50	0.55	0.54	–	0.42	1.75	–	1.30	–	–	–	[50]

[a]Silica–Alumina

[b]Calcium–silica–alumina

[c]Iron–silica or iron–alumina

[d]Silica

Influence of special additives

As listed in Table 1, various additives were used to produce artificial aggregates, and such additives enhance the properties of artificial aggregates. Adding $Ca(OH)_2$ has improved pelletization efficiency (52% to 99%) and reduced pelletization duration from 15 to 9 min. It is attributed to enhanced nuclei formation leading to a better agglomeration process and improved coagulation between the particles and specific area of the mix, thereby increasing pellet growth. Strength and bulk density also improved by adding $Ca(OH)_2$ [21, 34]. The borax was added mainly to enhance the aggregate's strength by inducing the aggregates' melting during the hardening process, which accelerates the melting material, resulting in increased strength [5]. Manganese dioxide (MnO_2) is a reactive oxide that reacts with sodium silicate in the case of alkali-activated aggregates production and improves density resulting in strong bonding and strength enhancement [34, 59].

Properties of artificial aggregates

Artificial aggregates exhibit variation in their behavior based on their composition and manufacturing process. The physical and mechanical properties and morphological characteristics make artificial aggregates unique from conventional aggregates. The variation in the properties of these aggregates is represented in Table 3.

Morphology

Morphological characteristics of aggregates are determined by size, shape, texture, surface, internal structure, and color. The shape of AAs changes with the production method, which influences concrete's qualities. The surface texture of AAs is either smooth or rough depending upon the precursors and hardening agents used, and the hardening method adopted. The color of AAs changes with the color of the binder and the hardening process [60–62].

Table 3 Properties of artificial aggregates

SG-OD[a] [SG-SSD][b]	LBD[c] [CBD][d] (g/cm^3)	WAB[e] (wt%)	ICS[f] (MPa)	ACV[g] [CRV][h] (%)	AIV[i] (%)	TPFV[j] (Tons)	Refs.
1.76–1.99	1.01–1.07 [1.13–1.55]	3.95–7.4	2.2–5.1	–	–	–	[3]
1.62–1.71	1.05–1.11 [1.17–1.22]	9.04–12.44	3.04–3.81	23.37–28.72	22.78–28.74	–	[6]
–	[0.90–1.24]	0.8 (1 h)	27.11 (bulk)	–	–	–	[1]
–	[1.00–1.13]	9.8–12.1	1.46–6.18	–	–	–	[35]
–	0.70–0.78	15–24.5	0.9–4.7	–	–	–	[16]
–	[1.80–1.85]	22–23	–	[60–61.4]	–		[36]
–	(0.80–0.87)	18.73–30.09	–	–	29–30	47–105	[2]
–	(1.81–1.98)	23.69–32.8	–	[44.03–61.59]	–	–	[37]
–	–	6.1	11.9 (bulk)	–	–	–	[38]
1.44–1.63	[0.92–1.02]	19.8–26.5	4–7.13	–	25.5–42.5	–	[39]
–	[0.90–2.0]	9–39	10–61[C]	–	–	–	[40]
1.94–2.02	–	6.6–12.40	2.87–4.01	–	23.50–27.57	–	[41]
–	[0.4–1.25]	–	2.5–28.4 [C]	–	–	–	[42]
–	–	5.0–12.9	2.3–3.9	–	19.2–30.2	–	[31]
–	[0.88–1.14]	32.8–52.0	2.04–2.66	–	–	–	[11]
1.42–1.44	0.80–0.78 [1.42–1.44]	18.19–19.14	–	–	–	–	[7]
1.63	–	11.5	–	–	–	–	[68]
–	[0.83–0.92]	17–25	5.64–9.93	–	–	–	[4]
–	–	–	0.87–17.5	–	–	–	[10]
1.2–2.0	0.95–1.11 [1.07–1.20]	16–21	6.15–8.32	–	–	–	[26]
	[1.0–1.60]	7.3–13.7	1.3–6.2	–	–	–	[12]
1.10–1.18	–	4.7–7.8	–	–	15.42–27.40	–	[43]
	–	10–22	–	–	–	–	[24]
1.11–1.78 [1.51–2.10]	0.67–1.0	12.88–32.89	16.39–23.76	–	–	–	[44]
–	0.768–0.869	5–22.3	0.85–1.47	–	–	–	[69]
–	[0.58–0.96]	22–52	–	–	–	5.2	[21]
1.53–1.62 [1.68–1.89]	0.848–0.983 [0.987–1.052]	13.01–21.26			31.96–50.47		[33]
–	0.57–1.10	–	–	–	–	5.5	[5]
1.44–1.75 [1.75–1.98]	0.867–1.03 [0.88–1.12]	13.01–21.26	3.43–22.81	–	31.96–50.47	–	[23]
–	[1.85–1.98]	3–23	0.6–7.4	–	–	–	[45]
–	[1.1–1.89]	1–44	10–892.41 N	–	–	–	[46]
–	[0.71–1.15]	10.3–12		–	–	1–4	[34]
–	[1.12–1.65]	15–19	1.8–6.0	–	–	–	[47]
2.06–2.86	[0.76–1.06]	7.8–20.5	15–31.2 kgf, 5.7–15.7	–	–	–	[22]
1.55–2.15 [1.86–2.25]	–	7–17.6	30–1010 N	–	–	–	[2]
1.12–1.95 [1.64–2.12]	0.60–0.94 [0.65–1.01]	12.77–77.03	0.55–13.78	–	–	–	[32]
–	[1.18–1.34]	11–13.5	1.9–4.5	–	–	–	[49]
1.34–1.93	–	0.7–18.4	5.1–20.4	–	–	–	[29]
–	0.6–0.9 [1.2–1.7]	12–25	0.8–8.0	–	–	–	[51]
–	–	15–24	1.65–2.8	–	–	–	[52]
1.55–1.61 [1.59–1.69]	[0.848–0.862]	2.4–3.4	–	26–28	–	–	[70]
1.72–1.79	–	–	–	–	–	–	[27]
–	–	3–27	50–860 N	–	–	1.1–1.78	[15]
1.6–1.76	–	21.3–35	–	–	–	–	[53]
–	0.63–0.98	4.5–17.7	–	–	–	–	[71]
–	[1.34–1.49]	26–28.2	–	–	–	–	[72]
[2.1]	1.076	13.7	5.32		16		[73]
	0.841	10.3	5.2		28.7	–	[74]

Table 3 (continued)

[a]Oven-dried specific gravity [b]surface saturated specific gravity [c]loose bulk density [d]compacted bulk density [e]water absorption [f]Individual aggregate crushing strength [g]aggregate crushing value [h]crushing resistance value [i]aggregate impact value [j]ten per cent fines value

For instance, fly ash aggregates were dark in color due to fly ash's dark color, and the aggregates produced by using red mud were reddish [1]. The fly ash-based geopolymer aggregates were dark gray before curing due to fly ash's dark color, and after curing, they turned slightly darker [63]. In the case of sintered aggregates, color has changed with the sintering temperature [40]. Lastly, considering the size and internal structure, the size of the produced AAs varies between 8 and 20 mm, with an average size of 13 mm. By visual observation, the internal structure showed spherical-shaped macro pores along with several micropores [60, 64].

Specific gravity and bulk density

As mentioned in Table 3, the majority of artificial aggregates exhibited a compacted bulk density and a loose bulk density of less than 2.0 g/cm^3 and 1.2 g/cm^3, respectively. The oven-dry and saturated surface dried specific gravity lie between the range of 1.10–2.0 and 1.51–2.25, respectively. Hence, produced artificial aggregates were classified as lightweight aggregates (LWA) as per UNE-EN-13055–1 (2003) [8, 51, 62, 64]. The specific gravity and bulk density of pelletized aggregates depend significantly on the binder content, curing regime, grain size, and sintering temperature [3, 25, 39, 40, 51]. The aggregates produced with fly ash of higher specific surface area and surface-treated aggregates showed higher specific gravity values [27]. The specific gravity and bulk density increase with the binder content [29, 39, 65, 66], and among the binders, aggregate with bentonite has shown lower specific gravity and bulk density than lime and cement [53]. Considering the curing regime, the bulk density of ambient cured aggregates is less than heat-cured and solution-cured aggregates [3], and it is higher when subjected to water curing [65]. The bulk density of aggregates also increases with the grain size due to the formation of voids among the particles [51, 67].

In the case of sintered aggregates, the bulk density decreased with an increased temperature (950 °C–1100 °C) due to bloating effect, removal of internal moisture, calorification, and combustion of organic materials [1, 25, 29, 40]. However, it raised to a higher value at a temperature of 1150 °C due to shrinkage [25, 40]. At low sintering temperatures, the aggregates produced with binders showed high specific gravity, which is attributed to an incomplete reaction resulting in deficient gas evolution to form pores within the pellets [29, 75].

Water absorption

The water absorption of aggregates influences the workability of the concrete; as listed in Table 3, it ranges between 0.7 and 32.8% for 24 h of immersion. The water absorption of aggregates decreases with the increased binder content [23, 32, 39, 48, 75], and among the binders, the cement is more effective, followed by clay minerals and lime [39, 49, 53]. In the case of sintered aggregates, the water absorption reduces with the increased sintering temperature and duration due to the formation of a vitrified surface along with a denser crystalline matrix facilitated by filling voids with melted compounds [5, 29, 46, 51, 76–78]. In alkali-activated aggregates, the water absorption decreased with increased molarity of NaOH due to enhanced microstructure [34, 44]. An increased water glass content (Na_2SiO_3) has also decreased water absorption [79]. It is also reviewed that the aggregates produced by employing a two-step pelletization process have substantially reduced the porosity of the outer part of the matrix than the single-step pelletization process [12]. From the above discussions, it is evident that artificial aggregates absorb substantially more water than natural aggregates. However, it is comparable with processed natural aggregates like scoria, pumice, and expanded clay [80]. It is also noted that artificial aggregates demand additional water during the mixing process to form fresh concrete with good workability [81].

Crushing and impact strength

Individual aggregates' mechanical behavior influences concrete's physical characteristics as it occupies the majority volume. The crushing strength of the aggregates depends on the binder content, curing regime and age, and pelletization factors. It also depends on interrelated factors such as aggregates' density, size, and shape [51]. Aggregate crushing resistance/TPFV increases with curing age and binder content due to the development of a denser microstructure and a strong bond between the particles and matrix [4, 53]. The increased pelletization duration improved aggregate strength [44], and accelerated curing with increased duration also positively influenced aggregates' crushing strength [52]. Considering the size, the smaller fraction (4–12 mm) of aggregates are less porous/denser. They exhibit higher crushing strength than the coarser ones due to the size effect and high porosity in bigger-sized aggregates [12, 25, 32].

It is also reviewed that the aggregate surface treated with soluble glass or water glass showed a particular improvement

in strength because water glass enhances hydration by consuming CaO and reacts with $Ca(OH)_2$ to form C–S–H. Additionally, it enters into the aggregate shell and repairs surface cracks. The combined effect of these factors resulted in a more robust and impermeable outer shell [27]. In the case of sintered aggregates, the compressive strength increases with an increase in sintering temperature from 900 °C to 1200 °C, and 1100 °C temperature is optimum to produce high-strength sintered artificial aggregates [42]. It was also reported that the source and composition of raw material influence the strength properties. For instance, the aggregates produced using pond ash of a bituminous source exhibited higher TPFV than pond ash of a lignite source. This can be attributed to the source material containing a higher amount of silica (SiO_2) and alumina (Al_2O_3), which led to the formation of solid ceramic bonding during sintering [5].

The strength of geopolymer aggregates improves by adding an alkali activator, as it promotes the hardening process by accelerating polymerization to form an alumino-silicate gel [24, 25]. The aggregates subjected to heat and solution curing have exhibited higher strength than ambient curing [3]. However, the strength gained in hot oven curing is more efficacious due to enhanced polymerization [32]. The crushing and impact strength also increased with the increased Na_2O content in the alkaline solution and curing duration [31, 43]. With the increase in molarity, fluid–binder ratio, and Na_2SiO_3–NaOH ratio, an increase in strength (TPFV) was observed, which is attributed to more reaction products formed due to enhanced polymerization [34, 43]. Besides, the fluid–binder ratio of 1.5 and the molarity of 12 M were considered optimum for producing alkali-activated aggregates with high strength values [63]. It was also noticed that the increased replacement level of GGBS with FA had improved strength because of enhanced dissolution of precipitation of C–S–H gel due to alkali activation of GGBS. On the contrary, an increase in RHA's replacement level would subside the strength of the aggregates [22]. Lastly, the crushing and impact strength of pelletized artificial aggregates satisfied the requirement for structural applications as per IS: 2386 (Part IV)-1963 [24, 25].

Application of artificial aggregates in concrete

Table 4 summarizes the mix proportions and properties of concrete containing artificial aggregate studied by various researchers. The following section discusses the influence of artificial aggregates on the overall performance of concrete.

Fresh properties of concrete

In general, the workability of concrete has been influenced by the size, shape, texture, and water absorption of aggregates, and also it depends on the water–binder ratio. As the size of the particle decreases, the specific surface area increases, requiring higher water content or superplasticizer dosage to attain workability [7, 50, 82]. But adding super plasticizing admixtures in higher dosages will affect the production costs. In artificial aggregate concrete, a lesser dosage of superplasticizer and the air-entraining agent is sufficient to achieve good workability over conventional concrete due to the rounded shape of aggregates [83, 84]. For the same water–binder ratio, the artificial aggregates of rounded shape produce more workable concrete than the conventional angular-shaped aggregates [50, 73, 85–87], which is attributed to reduced inter-particle aggregate friction offered by the free water present around the aggregates [25]. The LWAs absorb more water due to the presence of open pores resulting in a considerable impact on the strength of concrete; however, the LWAs of good quality with a layer of burning shell and compact structure reduce the water absorption and possibility of crushing during the mixing process [7]. The concrete substituted with ST-AA has exhibited more workability than CB-AA since aggregates pre-wetting consume less water [25].

The concrete incorporated with artificial aggregates has depicted a lower density than conventional concrete due to artificial aggregates of lower density [84, 88, 89]. The concrete's density can be reduced by up to 20% by utilizing LWA [84]. As mentioned in Table 4, the oven-dry density of concrete is less than 2000 kg/m^3. Hence, it has been categorized as a lightweight concrete (LWC).

Pumpability

Fresh concrete exhibits non-Newtonian fluid properties with heterogeneous composition. Pumping of concrete is a friction flow, and during pumping, shear stress is linearly distributed along the radius at each point of the cross section. Pumpable concrete comprises bulk concrete and a lubrication layer, which determines the pumping characteristics later. Pumping of concrete depends on concrete composition (binder, fine and coarse aggregate characteristics), workability, temperature, thixotropy, and lubrication layer [90]. Water absorption by LWA creates slump loss and low workability, which can be addressed by compensating for additional water [91, 92]. In USA water-saturated aggregates are used, and in Europe, pre-wetted aggregates are used to suit the pumping characteristics of concrete [93].

An advanced study on the pumping of LWC by Tima et al. [94] depicts the challenges of pumping. LWC is utilized in constructing exterior monolithic walls because of its

Table 4 Properties of artificial aggregate concrete

Cement (kg/m^3)	Fine aggregates (kg/m^3)		Coarse aggregates (kg/m^3)		SCMs[a]	Ac[b] %	Water (kg/m^3)	SP[c] % Vol Kg/m^3	W/B[d]	ODD[e] [SDD][f] (kg/m^3)	CS[g] (MPa)	TS[h] (MPa)	FS[i] (MPa)	E[j] (GPa)	Slump (mm)	Refs.
	F-AA[k]	F-NA[l]	C-AA[m]	C-NA[n]												
440	660	–	–	–	–	–	207 g	–	–	–	24	–	–	–	–	[2]
0	660	–	–	–	FA GGBS	–	–	–	–	–	7	–	–	–	–	[2]
371	–	684	686	–	–	–	163	0.25%	0.44	–	33.38	4.15	6.28	17	–	[95]
445	–	617	690	–	–	–	178	0.25%	0.40	–	50.58	5.01	6.36	22	–	[95]
425	–	878	395	–	–	–	170	–		1890	16.1	–	–	–	–	[39]
612	–	323	198–254	–	MK	–	235	4.83	0.25	1880	57.5–71.5	3.4–3.6	–	28.2–28.8	–	[7]
612	–	321	197–253	–	SF	–	235	5.17	0.25	1870	58–77.5	3.4–3.6	–	27.2–28.8	–	[7]
360		995	265	455	–	–	180	7	0.5	2179	48.9	–	–	–	–	[66]
400		690	408	605	–	–	262	–	0.65	1700	23	2.7	3.38	–	82	[83]
500 (only FA used)	–	1.5 × FA	1.1 × FA	–	FA	–	A/FA[o] = 0.4	Na_2SiO_3/NaOH = 2.5, SP = 1.9%		1835 [1951]	35.8	2.59	5.5	–	245	[68]
250	–	720	1070	–	–	–	112.5	–	–		20–28	2.18	–	16.23	–	[26]
350	Sand: AA = 3:4				–	–	175	–	–	1680–1970	18–34	–	–	23.6–27.3	65	[12]
358.6	–	693.1	732.6	–	–	–	125.5	1.5%	0.35	1909.8	27.8–41.3	2.4–2.5	3.3–4.3	19.4–22.1	63–76	[25]
35% of Vol	25% of Vol	25% of Vol	40% of Vol	50% of Vol	–	–	–	1.1–1.2%	0.40–0.45	1830–1905	28.87–52.64	–	2.62–4.45	31.3–36.7	–	[24]
310	–	708	851	–	–	–	–	3.6–5.7	0.5	1865.5–1981.4	22.5–41.8	–	–	–	–	[45]
353	–	904	388	–	FA	–	145	1.14%	0.30	1947	49.46	–	–	–	260	[46]
385	–	789	504	–	FA	–	165	6.1%	0.30	1971 [2053]	44.51	3.67	–	28.64	130	[96]
439.9	–	777.1	570.1	–	FA	–	164	0.8%	0.30	1992	21	–	–	–	270	[22]
400	–	800	635.7–738.2	–	–	–	200	2	0.5	[1976–2076]	28–50	–	–	–	–	[48]
352	–	838	595	–	–	6	155	–	0.45	–	26.7	–	–	–	–	[59]
549	–	634	580	–	SF	4.1	157	6.7	0.28	1943 [1975]	55	4.9	–	26	165	[50]
546.9	–	857.7	465.1	–	–	–	191.4	9	0.35	[2070]	60	–	–	28	200	[27]
402.7		908.1	475.2	–	–	–	221	2.5	0.55	[2010]	38	–	–	19	200	[27]
1.0 (wt. proportion)	–	2.23 × wt. of OPC	2.52 × wt. of OPC	–	–	–	–	–	0.53	–	33	–	–	–	95	[71]
1.0 (wt. proportion)	–	2.23 × wt. of OPC	2.20 × wt. of OPC	–	–	–	–	–	0.53	–	41	–	–	–	50	[71]

Table 4 (continued)

Cement (kg/m^3)	Fine aggregates (kg/m^3)		Coarse aggregates (kg/m^3)		SCMs[a]	Ac[b] %	Water (kg/m^3)	SP[c] % Vol Kg/m^3	W/B[d]	ODD[e] [SDD][f] (kg/m^3)	CS[g] (MPa)	TS[h] (MPa)	FS[i] (MPa)	E[j] (GPa)	Slump (mm)	Refs.
	F-AA[k]	F-NA[l]	C-AA[m]	C-NA[n]												
358.62	–	693.10	715	–	–	–	125.52	1.5%	0.35	[1892.2]	16.01	1.54	2.77	–	61	[33]
358.62	–	693.10	725	–	–	–	125.52	1.5%	0.35	[1902.2]	15.94	1.81	2.98	–	62	[33]
340	–	596 + 119 FA as fine aggregate	886	–	–	–	172.3 (Water + SP)	0.5%	0.38	–	34	–	–	–	85	[73]

[a]Supplementary cementitious materials

[b]Air content

[c]Superplasticizer

[d]Water–binder ratio [e]oven dry density [f]saturated dry density

[g]Compressive strength

[h]Tensile strength

[i]Flexural strength [j]elastic modulus

[k]Artificial fine aggregates [l]natural fine aggregates

[m]Artificial coarse aggregates

[n]Natural coarse aggregates

[o]Alkaline activator/fly ash

low density, enhanced thermal insulation with good robust behavior. For this purpose, pumping is an essential part affected by lightweight aggregates' characteristics. LWA bears interconnected open and closed pores, influencing the water content during mix design. High water absorption by LWA will suck water from cement paste, causing stiffening of concrete, which in turn causes choking of concrete pumping pipes. This can be addressed by pre-wetting LWA, using water-reducing admixtures, or making LWA non-porous. The prime challenges in the pumping of LWC are.

1. Pressurizing concrete will squeeze cement paste into porous LWA, which reduces the flowability of concrete and increase friction inside the pipe.
2. As water is forced into LWA during pumping, it might lead to a loss of volume, which makes the concrete elastic and pumpable during pumping.
3. Once the concrete ooze out of the pumping pipe, compressed air within LWA will liberate water into the concrete matrix, which might cause segregation.

Mechanical properties of hardened concrete

Compressive strength

Table 4 shows that the compressive strength of concrete incorporated with artificial aggregates has ranged from 15.94 to 77.5 MPa. The artificial aggregates produced using the sintering and alkali-activation technique are proved to be adequate for obtaining LWC with performances comparable to that of normal-weight concrete (NWC) [24]. The compressive strength of LWC depends significantly on the properties of LWA, such as specific gravity, porosity, water absorption capacity, crushing strength, and particle size distribution [48]. It also depends on the water–binder ratio, volume of artificial aggregates used in the mix, and curing regime employed [25, 26, 33, 96]. The addition of mineral admixtures positively influences the concrete's compressive strength due to their pozzolanic and densification action [7]. It is also reviewed that the concrete containing artificial aggregates has depicted lesser compressive strength than NWC due to the inferior properties of artificial aggregates [22, 50, 96]. The concrete incorporated with ST-AA exhibited improved strength than the concrete with CB-AA, which is attributed to the higher porosity and lower strength of CB-AA [25]. Similarly, the concrete produced with surface-treated aggregates has shown a 30% enhancement in compressive strength compared to non-treated aggregates [27].

Split tensile and flexural strength

Table 4 shows the split tensile and flexural strengths of artificial aggregate concrete produced by various researchers, which range from 1.54 to 4.01 MPa and 2.12 to 5.5 MPa, respectively. These properties are proportional to the compressive strength and might vary according to the specific behavior of ingredients and additives. The tensile strength of concrete significantly depends on the tensile properties of aggregate, paste matrix, and interfacial transition zone (ITZ) [97], and it increases with the increased duration of curing, mortar, and aggregate strength [26, 68]. The concrete containing an increased volume of artificial aggregates has shown a decrement in the tensile strength due to the plane of failure originating in the artificial aggregates. Hence, it clearly reveals that the concrete's tensile properties depend more on the properties of mortar than on aggregates due to the establishment of maximum diametric tension in the concrete specimen, which causes the diametric splitting of concrete [25]. LWA has a lesser surface area, less angular shape, and low surface roughness, which might result in lesser strengths in the aggregate transition zones than the normal-weight aggregates (NWA) [24].

The flexural properties of concrete were similar to split tensile strength. The matrix densification and reduced volume of artificial aggregates in the mix have improved the flexural properties of concrete. The flexural properties of LWC depend more on the mortar properties, and the contribution of artificial aggregates in exhibiting resistance to flexural bending is negligible. For instance, the higher flexural elastic modulus during bending has resulted from the increase in mortar volume, which has compensated for the decrease in aggregate volume [25].

Modulus of elasticity

As mentioned in Table 4, the modulus elasticity (MoE) of LWC ranges between 16.23 and 28.8 GPa. The artificial aggregates are typically weaker than the mortar phase, aggravating concrete's mechanical properties when used at a higher volume [98, 99]. However, an improvement in the aggregate crushing strength furnished by surface treatments, special additives, or binders remarkably reduced this adverse effect of artificial aggregates in both modulus of elasticity and compressive strength [27]. The MoE of concrete is proportional to compressive strength. However, there is uncertainty on the precise relationship between them because the MoE of the concrete is influenced by the MoE of aggregates and the volumetric proportion of aggregate in the concrete [96]. The MoE of LWC increases with the mortar and aggregate strength [26], and it depends on the density, total porosity, surface texture, pore structure, and critical pore diameter of LWA [50]. The MoE of artificial aggregate concrete is lower than the MoE of conventional concrete, which is attributed to higher porosity, lower strength, and lower MoE of aggregates [96]. The sintered aggregates formed dense microstructure, more refined and uniformly distributed pores compared

to cold-bonded aggregates, and incorporation of these in concrete led to improvement in MoE [50]. The addition of SCMs does not have a role in improving the MoE due to the lower stiffness contributed by the artificial aggregates in concrete [7]. It is also reviewed that the artificial aggregates produced by the pelletization process form a surface with craters, which is essential for the function and adequacy of aggregates. Additionally, it enhances the bonding property of aggregate with cement paste matrix resulting in increased strength and MoE [70].

Mode of failure

The concrete failure modes can be attributed as failure in between bonding, failure on bonding, and failure on aggregate. In normal aggregate concrete, the failure mostly happened in between bonding and on bonding because the aggregates were denser and stronger. The failure mode of concretes made with artificial aggregates under axial compression was similar to the natural aggregate concrete. However, the failure on aggregate more often occurs, which might be due to the lower density and lower specific gravity of LWA as compared with natural gravel [100].

Ultrasonic pulse velocity

The pulse velocity test is an actual non-destructive test (NDT), which evaluates the strength of the concretes based on the cracks and voids present in the matrix and the quality packing of the aggregate-mortar interface [83, 101, 102]. The pulse velocity of concrete containing artificial aggregates is lower than natural aggregate concrete in all curing ages. It decreases with the increased volume of artificial aggregates due to increased porosity and the formation of more voids and microcracks [75, 83, 100]. However, the pulse velocity of all the concrete mixes containing artificial aggregates was in the range of 3.42–4.51 km/s; hence, it was considered as good as per IS: 13311 (part 1) [83, 102].

Rebound hammer test

This NDT provides the compressive strength of the concrete with respect to the rebound number depicted by the rebound hammer, which is dependent upon the density of the matrix. The rebound number for concrete containing LWA and conventional concrete is comparable. In a study, the rebound number for conventional concrete was 34, whereas for the LWC, it ranges between 25 and 33. A minor decrement in rebound number for LWC might be due to the porous nature of LWA [83].

Microstructure of artificial aggregate concrete

Concrete's mechanical behavior and durability depend on cement paste, aggregate, and the interfacial zone between them [103–105]. A weak interfacial zone will seriously affect durability because it allows water and harmful ions to quickly enter the concrete, deteriorating the concrete and the reinforcement. The ITZ between the natural aggregate and the hardened cement paste (HCP) is porous due to the "Wall Effect" or "Surface Effect" occurring at the surface of the natural aggregate. In LWA concrete, cement paste will penetrate the surface pores of the LWA to some depth and avoid the "Wall Effect" on the ITZ, leading to reduced porosity. The surface pores provide the interlocking site for cement paste to form a better interfacial bond at the ITZ, resulting in much higher initial strength than the natural aggregate concrete [62, 103, 104, 106]. Enhanced bonding is also noticed for the water absorption by the LWA from the neighboring paste. It is also reviewed that concrete containing artificial aggregates exhibits high resistance against sulfate attack, sorptivity, and electrical conductivity due to the surface pores of the AAs will be sealed by the dense cement paste [107]. The high porosity of the LWA does not appear to increase the transport properties as it is sealed by the dense ITZ [107, 108]. It is also found that as the FA content in LWC increases, the amount of paste also increases, resulting in a higher distribution of paste into the surface pore of the aggregates forming a dense microstructure, which leads to improved strength and transport properties. In addition, an increased FA content in concrete has contributed to early strength gain due to its pozzolanic activity inducing the formation of a higher amount of C–S–H by consuming large $Ca(OH)_2$ [109, 110]. Lo et al. reported that the increase in pore area percentage at the ITZ significantly affects the concrete strength. The higher water absorption of AAs makes the ITZ more porous, resulting in strength decrement [111], which contradicts the above discussions.

Figure 4 reveals that the cold-bonded aggregates exhibit enhanced bonding with time. Due to artificial aggregates' porousness and the availability of reactive pozzolana at the surface, the ITZ experiences surface interaction [110] and forms a firm bonding with the aggregate. However, Fig. 5 shows that the cold-bonded aggregate's surface is smooth, and its interaction with the ITZ is less than sintered aggregates as the surface of sintered aggregates is porous due to thermal input.

Durability properties of artificial aggregate concrete

Various internal and external factors govern the durability of concrete. Internal factors refer to the characteristics exhibited by the concrete because of its internal structure, whereas

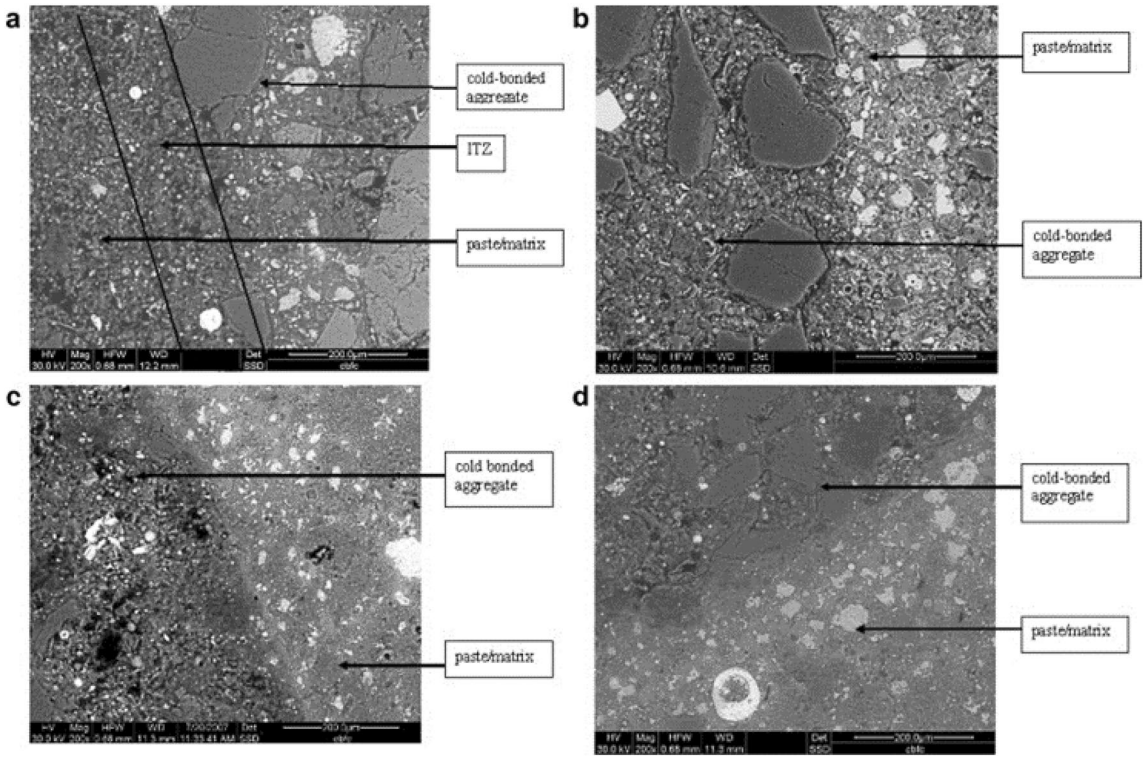

Fig. 4 Bonding stages of artificial aggregates with mortar matrix [110]

Fig. 5 Bonding of (a) CB-AA and (b) ST-AA [66]

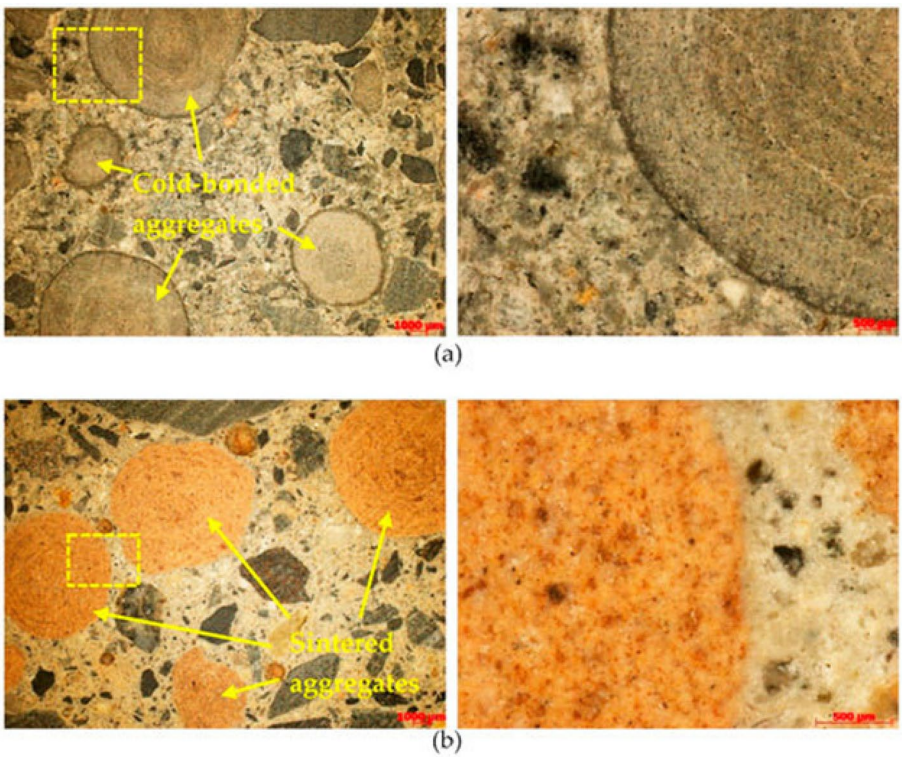

external factors refer to the exposure conditions. The various factors affecting the durability are explained as follows.

Sorptivity

Sorptivity represents the tendency of a porous material to absorb and transmit water by capillary action. In comparison to conventional concrete, artificial aggregate concrete showed higher sorptivity values. However, the values were within acceptable bounds, which suggests that the concrete is durable in terms of sorptivity [95, 112]. The sintered aggregates are less porous and have a well-developed microstructure than cold-bonded aggregates, which results in less water absorption. The concrete with increased content of artificial aggregates depicted increased sorptivity due to a larger exposed area of aggregates. Ultimately, it showed the circulation of more capillary water through the aggregate pores. Hence, it can be subsided with the reduction in artificial aggregate volume [25].

Porosity

The interlinked pores or microcracks within the concrete matrix cause the porosity of concrete. Regardless of the concrete's grade, concrete produced of sintered aggregate showed complete water absorption at the mid-length compared to the conventional mix. The aggregates' porous nature causes this effect. When the quality criteria of the concrete are not carefully followed, it may result in corrosion and other related issues [95].

Chloride migration

A rapid chloride penetration test determines the migration of chloride ions within the concrete matrix. The chloride penetration resistance in LWC and NWC is enhanced with the curing age and reduced water–binder ratio. Also, it depends on the type of binder used in the matrix [7, 73, 96, 113]. In artificial aggregate concrete, curing age has more influence than binder type and water–binder ratio; as the curing duration lengthens, chloride penetration reduces due to the refinement of the pore structure. The addition of mineral admixtures further reduces chloride permeation; especially SF and FA showed a beneficial influence on chloride penetration due to high specific surface area and pozzolanic activity, respectively, which leads to the densification of pore structure [7, 73, 96]. Concrete with cold-bonded aggregates has shown higher chloride penetration than concrete with sintered and natural aggregates, which is attributed to the higher porosity and absorption of cold-bonded aggregates [50]. The concrete with sintered aggregates exhibited lesser permeability than the natural aggregate concrete due to the formation of superior ITZ by penetrating paste into the surface pores of aggregates [7, 50, 113]. The chloride-ion migration for LWAC and NWAC are comparable due to the limited ingress of chloride-ion through LWA due to their dense shell structure [112].

Carbonation resistance

Carbonation occurs due to the reaction between the available moisture and the carbon dioxide (CO_2) at the surface of the concrete. The carbonation depth or rate of carbonation depends on the duration of time concrete is exposed to CO_2. Concrete containing artificial aggregates showed carbonation depths of not more than 1 mm, which was possibly caused by the interfacial pore refinement. These artificial aggregates enable internal curing, extend the curing process further, and help to form superior ITZ within the concrete matrix, resulting in higher resistance against carbonation similar to NWC [7].

Corrosion rate

The movement of ions mainly governs the corrosion of reinforcement in the concrete through the concrete matrix containing moisture. The addition of SCMs during the production of NWC and LWC improves the pore structure and influences pore solution composition, resulting in enhanced corrosion resistance. The SCMs, especially the silica fume, provides better corrosion resistance than metakaolin in initial ages due to their high specific surface area, which facilitates enhanced pozzolanic action and voids filling ability. The effectiveness of SCMs is higher in concrete, having a lower water-binder ratio (0.25). Hence, it is recommended to use sintered aggregates and mineral admixtures to produce good-quality concrete in an aggressive environment [113] [7].

Dry shrinkage

The shrinkage in the concrete matrix might lead to microcracks due to the stress formed along the matrix, which might further act as the path for the ingress of moisture or chemicals for the deterioration. The concrete containing artificial aggregate exhibited a higher drying shrinkage, while the concrete containing natural aggregate exhibited a lower drying shrinkage [114]. The shrinkage in both NWC and LWC can be reduced using SCMs and employing a lower water–binder ratio. The concrete containing SCMs usually attains stability against shrinkage after long days (13 weeks) compared to conventional mixes without SCM due to the extended pozzolanic activity of SCMs [7].

Alternate wetting and drying

Alternate wetting and drying cycles measure concrete durability in terms of resistance against continuous weathering conditions. The concrete with ST-AA exhibited minimum weight loss compared to CB-AA after progressive wetting and drying cycles and suggested that ST-AA are more favorable in enhancing the durability of concrete. The concrete specimens tested on the initial days depicted minimum weight loss. At a later testing age, the weight loss gradually increased due to the deterioration of microstructure caused by the movement of water through pores [25].

Sulfate attack

The concrete's sulfate reactivity is a key indicator of strength loss due to the reaction between sulfate ions and hydration products, which results in the formation of gypsum and ettringite. The concrete containing low-volume CB-AA presented maximum strength loss compared to concrete with the same volume of ST-AA. However, the minimum strength degradation was noticed in concretes containing a high volume of CB-AA and ST-AA. This is primarily because a decrease in cement content causes a decrease in the amount of the hydration product $Ca(OH)_2$, which in turn causes a decrease in the volume of ettringite to form. The formation of the microstructure and resistance to volume changes in concrete are further factors that affect the sulfate resistance of the concrete [25].

Freezing and thawing

The freezing and thawing test determines the concrete durability in terms of resistance against frost. The CB-AA have shown poor performance against freezing and thawing cycles at 28 and 56 days compared to ST-AA. This is primarily caused by the larger voids or pores in CB-AA, which increase the amount of water that can freeze and the saturation level of the concrete [50]. When using water-saturated aggregates (24 h of water absorption) at the time of mixing, lightweight concrete's resistance to freezing and thawing is decreased because the concrete becomes considerably more saturated and experiences damage much more quickly during the freezing and thawing test [115]. NWC showed less resistance to freezing and thawing than concretes containing ST-AA due to the high level of protection offered by air entrainment for artificial aggregate concretes subjected to freezing and thawing conditions [50]. The limited study that was identified in the literature revealed that concrete containing artificial lightweight aggregates demonstrated good freeze–thaw resistance when 6% entrained air content was considered for design. The resistance was satisfactory when the concrete was designed for 4% entrained air content [50, 59]. In addition, the incorporation of mineral admixtures in concrete production further enhances the freeze–thaw resistance due to the formation of denser microstructure [50].

Water permeability and volume of permeable voids (VPV)

The NWC depicted lesser water permeability than the cold-bonded aggregate concrete, mainly due to lesser water absorption and lower open porosity of convention aggregates. The water permeability and porosity can be reduced with the increased binder content, which increases the hydration volume [73]. It is also highlighted that the smooth surfaces of artificial aggregates address water infiltration through the aggregate and mortar interface, resulting in weak bond strength with cement paste [116]. The concrete with sintered aggregates showed lesser water permeability than NWC, attributed to the aggregate's vitrified surface and fewer pores within the concrete [113, 117]. VPV is a crucial characteristic of concrete because it considerably influences the mechanism of harmful liquids and gases transported through the concrete. The VPV of cold-bonded alkali-activated aggregate concrete was marginally different from that of natural-weight aggregate concrete; however, permeable pores in cold-bonded lightweight aggregate concrete were a little higher as a result of the LWA's greater water absorption [118].

Alkali-silica reaction

The concrete containing LWA is less susceptible to the alkali-silica reaction (ASR) because the formed ASR gel can be accommodated in the pores of LWA, which reduces the expansion. Additionally, it was stated that the concrete produced using LWA and incorporating FA exhibits equivalent or lower expansion than natural aggregate concrete, irrespective of the matrix employed (cement or alkali-activated materials), which is attributed to the formation of dense bonds around aggregates. Moreover, alkalis in the pore solution are absorbed by FA, which uses them to form polymers, further decreasing ASR's danger [2, 18].

Summary and conclusions

In this article, different raw materials, binders, special additives, and methods for preparing artificial aggregates are reviewed and presented. The production process and the growth mechanism of aggregate through the pelletization process also have been highlighted. The pelletization factors influencing aggregates' production process and properties have been discussed. The properties and performance of concrete manufactured using CB-AA and

ST-AA have been elaborated. The broad implications that can be formed in light of the discussions mentioned above are as follows.

1. The pelletization process is a highly developed balling technique that includes nucleation and transition stages to produce artificial aggregates. The pelletization efficiency depends on the properties of raw materials, type and dosage of binder, as well as the size, shape, surface area, and wettability of particles, along with the speed and tilt-angle of the pelletizer.
2. The loose and compacted bulk density of all kinds of artificial aggregates would range between 0.60 and 1.11 g/cm^3 and 0.80–1.98 g/cm^3, respectively. Hence, they can be categorized as lightweight aggregates as per the standard codes.
3. The qualities of aggregates can be enhanced by incorporating special additives and alkali activators during mixing, surface treatment, adopting different curing regimes, or a multiple-step pelletization process.
4. The cement paste or hydration products penetrate the cavities or pores on the aggregate surface to form denser and homogeneous ITZ, resulting in an enhanced bond between aggregates and cement matrix, resulting in improved mechanical and transport properties.
5. Artificial lightweight aggregates in concrete achieve good workability without using superplasticizers and air-entraining agents due to their rounded shape. It can also achieve 20% less fresh density when compared to normal-weight concrete. Hence, fresh properties of artificial lightweight aggregate concrete are superior to that of normal-weight concrete.
6. Artificial aggregate concrete's mechanical properties are inferior to conventional concrete due to lighter aggregates' higher porosity and lower strength. However, it is feasible to use in both structural and non-structural applications.
7. Concrete made with sintered aggregates is more durable than concrete with cold-bonded aggregates due to lesser porosity and the refined microstructure shown by the sintered aggregates, which leads to lesser water absorption.

Thus, it can be concluded that lightweight artificial aggregates can be one of the best alternatives for conventional aggregates in the near future.

Future research objectives/challenges

From the overview of research, the following challenges and objectives were derived for future research.

1. There is a need for an eco-friendly alternative for cement-stabilized artificial aggregates, as cement production is proven to be eco-detrimental.
2. Selection of materials for making artificial aggregates, as their characteristics will influence the properties of aggregates and also govern the behavior of concrete.
3. Alkali-activated artificial aggregates can be a sustainable alternative to cement-based artificial aggregates. However, breaking the complexity of the molarity of the activator solution, fluid–binder ratio, material selection, and their optimum combination is a break-even point.
4. Suitable applications of artificial aggregates need to be explored
5. To understand the compatibility and durability of lightweight concrete, a detailed experimental approach to microstructure analysis is essential. It might provide insights into mechanisms and rheology in manufacturing lightweight concrete.
6. Limited studies on the adaptability of lightweight concrete as thermal insulating material to conserve energy.
7. Minimal data reported on the pumpability of lightweight aggregate concrete

Funding Open access funding provided by Manipal Academy of Higher Education, Manipal.

References

1. Sun Y, Li J, shan, Chen Z, Xue Q, Sun Q, Zhou Y, Chen X, Liu L, Poon CS, (2021) Production of lightweight aggregate ceramsite from red mud and municipal solid waste incineration bottom ash: Mechanism and optimization. Constr Build Mater. https://doi.org/10.1016/j.conbuildmat.2021.122993
2. Ul Rehman M, Rashid K, UlHaq E, Hussain M, Shehzad N (2020) Physico-mechanical performance and durability of artificial lightweight aggregates synthesized by cementing and geopolymerization. Constr Build Mater. https://doi.org/10.1016/j.conbuildmat.2019.117290
3. Shivaprasad KN, Das BB, Krishnadas S (2021) Effect of Curing Methods on the Artificial Production of Fly Ash Aggregates. In: Lecture Notes in Civil Engineering. Springer Science and Business Media Deutschland GmbH, pp 23–32

4. Tang P, Brouwers HJH (2017) Integral recycling of municipal solid waste incineration (MSWI) bottom ash fines (0–2 mm) and industrial powder wastes by cold-bonding pelletization. Waste Manage 62:125–138. https://doi.org/10.1016/j.wasman.2017.02.028
5. Vasugi V, Ramamurthy K (2014) Identification of admixture for pelletization and strength enhancement of sintered coal pond ash aggregate through statistically designed experiments. Mater Des 60:563–575. https://doi.org/10.1016/j.matdes.2014.04.023
6. Shivaprasad KN, Das BB (2021) Study on the production factors in the process of production and properties of fly ash-based coarse aggregates. Adv Civil Eng. https://doi.org/10.1155/2021/4309569
7. Nadesan MS, Dinakar P (2018) Influence of type of binder on high-performance sintered fly ash lightweight aggregate concrete. Constr Build Mater 176:665–675. https://doi.org/10.1016/j.conbuildmat.2018.05.057
8. Huang H, Yuan Y, Zhang W, Gao Z (2019) Bond behavior between lightweight aggregate concrete and normal weight concrete based on splitting-tensile test. Constr Build Mater 209:306–314. https://doi.org/10.1016/j.conbuildmat.2019.03.125
9. González-Corrochano B, Alonso-Azcárate J, Rodas M (2012) Effect of thermal treatment on the retention of chemical elements in the structure of lightweight aggregates manufactured from contaminated mine soil and fly ash. Constr Build Mater 35:497–507. https://doi.org/10.1016/j.conbuildmat.2012.04.061
10. Yliniemi J, Nugteren H, Illikainen M, Tiainen M, Weststrate R, Niinimäki J (2016) Lightweight aggregates produced by granulation of peat-wood fly ash with alkali activator. Int J Miner Process 149:42–49. https://doi.org/10.1016/j.minpro.2016.02.006
11. Tajra F, Elrahman MA, Chung SY, Stephan D (2018) Performance assessment of core-shell structured lightweight aggregate produced by cold bonding pelletization process. Constr Build Mater 179:220–231. https://doi.org/10.1016/j.conbuildmat.2018.05.237
12. Colangelo F, Messina F, Cioffi R (2015) Recycling of MSWI fly ash by means of cementitious double step cold bonding pelletization: technological assessment for the production of lightweight artificial aggregates. J Hazard Mater 299:181–191. https://doi.org/10.1016/j.jhazmat.2015.06.018
13. Manikandan R, Ramamurthy K (2007) Influence of fineness of fly ash on the aggregate pelletization process. Cem Concr Compos 29:456–464. https://doi.org/10.1016/j.cemconcomp.2007.01.002
14. Tajra F, Elrahman MA, Stephan D (2019) The production and properties of cold-bonded aggregate and its applications in concrete: a review. Constr Build Mater 225:29–43
15. Harikrishnan KI, Ramamurthy K (2006) Influence of pelletization process on the properties of fly ash aggregates. Waste Manage 26:846–852. https://doi.org/10.1016/j.wasman.2005.10.012
16. Xu LY, Qian LP, Huang BT, Dai JG (2021) Development of artificial one-part geopolymer lightweight aggregates by crushing technique. J Clean Prod. https://doi.org/10.1016/j.jclepro.2021.128200
17. Peyne J, Gautron J, Doudeau J, Rossignol S (2018) Development of low temperature lightweight geopolymer aggregate, from industrial Waste, in comparison with high temperature processed aggregates. J Clean Prod 189:47–58. https://doi.org/10.1016/j.jclepro.2018.04.038
18. Qian LP, Xu LY, Alrefaei Y, Wang T, Ishida T, Dai JG (2022) Artificial alkali-activated aggregates developed from wastes and by-products: a state-of-the-art review. Resour Conserv Recycl. https://doi.org/10.1016/j.resconrec.2021.105971
19. Barkate AR, Bothara SB, Mahaparale PR, Lohar PS, Tambade SB (2020) Methods of pelletization using extrusion—spheronization: a review. Int J Pharm Pharm Res 18:385–399. https://doi.org/10.25166/ijppr.2020.v18i01.029
20. Sirisha VR, Vijaya Sri K, Suresh K, Reddy GK, Devanna N (2013) A review of pellets and pelletization process-a multiparticulate drug delivery system. Int J Pharm Sci Res 4:2145–2158. https://doi.org/10.13040/IJPSR.0975-8232.4(6).2145-58
21. Vasugi V, Ramamurthy K (2014) Identification of design parameters influencing manufacture and properties of cold-bonded pond ash aggregate. Mater Des 54:264–278. https://doi.org/10.1016/j.matdes.2013.08.019
22. Bui LAT, Hwang CL, Chen CT, Lin KL, Hsieh MY (2012) Manufacture and performance of cold bonded lightweight aggregate using alkaline activators for high performance concrete. Constr Build Mater 35:1056–1062. https://doi.org/10.1016/j.conbuildmat.2012.04.032
23. Perumal G, Anandan S (2014) Performance evaluation of alkali activated fly ash lightweight aggregates. Eng J 18:77–85. https://doi.org/10.4186/ej.2014.18.1.77
24. Terzić A, Pezo L, Mitić V, Radojević Z (2015) Artificial fly ash based aggregates properties influence on lightweight concrete performances. Ceram Int 41:2714–2726. https://doi.org/10.1016/j.ceramint.2014.10.086
25. Gomathi P, Sivakumar A (2015) Accelerated curing effects on the mechanical performance of cold bonded and sintered fly ash aggregate concrete. Constr Build Mater 77:276–287. https://doi.org/10.1016/j.conbuildmat.2014.12.108
26. Thomas J, Harilal B (2015) Properties of cold bonded quarry dust coarse aggregates and its use in concrete. Cem Concr Compos 62:67–75. https://doi.org/10.1016/j.cemconcomp.2015.05.005
27. Gesoğlu M, Özturan T, Güneyisi E (2007) Effects of fly ash properties on characteristics of cold-bonded fly ash lightweight aggregates. Constr Build Mater 21:1869–1878. https://doi.org/10.1016/j.conbuildmat.2006.05.038
28. Vali KS, Murugan B (2019) Impact of nano SiO2 on the properties of cold-bonded artificial aggregates with various binders. International Journal of Technology 10:897–907. https://doi.org/10.14716/ijtech.v10i5.2590
29. Kockal NU, Ozturan T (2011) Characteristics of lightweight fly ash aggregates produced with different binders and heat treatments. Cem Concr Compos 33:61–67. https://doi.org/10.1016/j.cemconcomp.2010.09.007
30. Giro-Paloma J, Mañosa J, Maldonado-Alameda A, Quina MJ, Chimenos JM (2019) Rapid sintering of weathered municipal solid waste incinerator bottom ash and rice husk for lightweight aggregate manufacturing and product properties. J Clean Prod 232:713–721. https://doi.org/10.1016/j.jclepro.2019.06.010
31. Shivaprasad KN, Das BB (2018) Determination of optimized geopolymerization factors on the properties of pelletized fly ash aggregates. Constr Build Mater 163:428–437. https://doi.org/10.1016/j.conbuildmat.2017.12.038
32. Gomathi P, Sivakumar A (2012) Characterization on the strength properties of pelletized fly ash aggregate. ARPN J Eng Appl Sci 7:1523–1532
33. Gomathi P, Sivakumar A (2014) Synthesis of geopolymer based class-F fly ash aggregates and its composite properties in concrete. Arch Civ Eng 60:55–75. https://doi.org/10.2478/ace-2014-0003
34. Geetha S, Ramamurthy K (2013) Properties of geopolymerised low-calcium bottom ash aggregate cured at ambient temperature. Cem Concr Compos 43:20–30. https://doi.org/10.1016/j.cemconcomp.2013.06.007
35. Tian K, Wang Y, Hong S, Zhang J, Hou D, Dong B, Xing F (2021) Alkali-activated artificial aggregates fabricated by red mud and fly ash: Performance and microstructure. Constr Build Mater. https://doi.org/10.1016/j.conbuildmat.2021.122552

36. Risdanareni P, Schollbach K, Wang J, de Belie N (2020) The effect of NaOH concentration on the mechanical and physical properties of alkali activated fly ash-based artificial lightweight aggregate. Constr Build Mater. https://doi.org/10.1016/j.conbuildmat.2020.119832
37. Risdanareni P, Villagran Y, Schollbach K, Wang J, de Belie N (2020) Properties of alkali activated lightweight aggregate generated from Sidoarjo Volcanic Mud (Lusi), fly ash, and municipal solid waste incineration bottom ash. Materials. https://doi.org/10.3390/ma13112528
38. Dewa I, Karyawan A, Ekaputri JJ, Widyatmoko I, Ahyudanari E (2020) The effect of various na2sio3/naoh ratios on the physical properties and microstructure of artificial aggregates
39. Baalbaki O, Saad M, Baalbaki O, Khatib J, Kordi A el, Masri A (2019) Manufacturing of lightweight aggregates from municipal solid waste incineration bottom ash and their impacts on concrete. Debbieh, Lebanon
40. Chuang KH, Lu CH, Chen JC, Wey MY (2018) Reuse of bottom ash and fly ash from mechanical-bed and fluidized-bed municipal incinerators in manufacturing lightweight aggregates. Ceram Int 44:12691–12696. https://doi.org/10.1016/j.ceramint.2018.04.070
41. Shivaprasad KN, Das BB (2018) Effect of Duration of Heat Curing on the Artificially Produced Fly Ash Aggregates. In: IOP Conference Series: Materials Science and Engineering. Institute of Physics Publishing
42. Liu M, Wang C, Bai Y, Xu G (2018) Effects of sintering temperature on the characteristics of lightweight aggregate made from sewage sludge and river sediment. J Alloys Compd 748:522–527. https://doi.org/10.1016/j.jallcom.2018.03.216
43. Razak RA, Abdullah MMAB, Hussin K, Ismail KN, Hardjito D, Yahya Z (2015) Optimization of NaOH molarity, LUSI mud/alkaline activator, and Na2SiO3/NaOH ratio to produce lightweight aggregate-based geopolymer. Int J Mol Sci 16:11629–11647. https://doi.org/10.3390/ijms160511629
44. Gomathi P, Sivakumar A (2014) Cold bonded fly ash lightweight aggregate containing different binders. Res J Appl Sci Eng Technol 7:915–920. https://doi.org/10.1926/rjaset.7.365
45. Colangelo F, Cioffi R (2013) Use of cement kiln dust, blast furnace slag and marble sludge in the manufacture of sustainable artificial aggregates by means of cold bonding pelletization. Materials 6:3139–3159. https://doi.org/10.3390/ma6083139
46. Tuan BLA, Hwang CL, Lin KL, Chen YY, Young MP (2013) Development of lightweight aggregate from sewage sludge and waste glass powder for concrete. Constr Build Mater 47:334–339. https://doi.org/10.1016/j.conbuildmat.2013.05.039
47. Ferone C, Colangelo F, Messina F, Iucolano F, Liguori B, Cioffi R (2013) Coal combustion wastes reuse in low energy artificial aggregates manufacturing. Materials 6:5000–5015. https://doi.org/10.3390/ma6115000
48. Gesoğlu M, Güneyisi E, Öz HÖ (2012) Properties of lightweight aggregates produced with cold-bonding pelletization of fly ash and ground granulated blast furnace slag. Materials and Structures/Materiaux et Constructions 45:1535–1546. https://doi.org/10.1617/s11527-012-9855-9
49. Cioffi R, Colangelo F, Montagnaro F, Santoro L (2011) Manufacture of artificial aggregate using MSWI bottom ash. Waste Manage 31:281–288. https://doi.org/10.1016/j.wasman.2010.05.020
50. Kockal NU, Ozturan T (2010) Effects of lightweight fly ash aggregate properties on the behavior of lightweight concretes. J Hazard Mater 179:954–965. https://doi.org/10.1016/j.jhazmat.2010.03.098
51. González-Corrochano B, Alonso-Azcárate J, Rodas M (2009) Characterization of lightweight aggregates manufactured from washing aggregate sludge and fly ash. Resour Conserv Recycl 53:571–581. https://doi.org/10.1016/j.resconrec.2009.04.008
52. Manikandan R, Ramamurthy K (2008) Effect of curing method on characteristics of cold bonded fly ash aggregates. Cem Concr Compos 30:848–853. https://doi.org/10.1016/j.cemconcomp.2008.06.006
53. Ramamurthy K, Harikrishnan KI (2006) Influence of binders on properties of sintered fly ash aggregate. Cem Concr Compos 28:33–38. https://doi.org/10.1016/j.cemconcomp.2005.06.005
54. Ren P, Ling TC, Mo KH (2021) Recent advances in artificial aggregate production. J Clean Prod 291
55. Khan Baykal G, Gü A, Ven D (2000) Utilization of fly ash by pelletization process; theory, application areas and research results. Turkey
56. Criado M, Aperador W, Sobrados I (2016) Microstructural and mechanical properties of alkali activated Colombian raw materials. Materials. https://doi.org/10.3390/ma9030158
57. Gao X, Yu Q, Brouwers H Development of Alkali Activated Slag-Fly Ash Mortars: Mix Design and Performance Assessment
58. Hu Y, Liang S, Yang J, Chen Y, Ye N, Ke Y, Tao S, Xiao K, Hu J, Hou H, Fan W, Zhu S, Zhang Y, Xiao B (2019) Role of Fe species in geopolymer synthesized from alkali-thermal pretreated Fe-rich Bayer red mud. Constr Build Mater 200:398–407. https://doi.org/10.1016/j.conbuildmat.2018.12.122
59. Jo B, wan, Park S kook, Park J bin, (2007) Properties of concrete made with alkali-activated fly ash lightweight aggregate (AFLA). Cem Concr Compos 29:128–135. https://doi.org/10.1016/j.cemconcomp.2006.09.004
60. Zafar I, Rashid K, Ju M (2021) Synthesis and characterization of lightweight aggregates through geopolymerization and microwave irradiation curing. J Build Eng 42:102454. https://doi.org/10.1016/j.jobe.2021.102454
61. Czuryszkiewicz A, Paraisten Kalkki MO (1973) The effect of aggregate shape upon the strength of structural lightweight-aggregate concrete. Finland
62. Kwek SY, Awang H, Cheah CB, Mohamad H (2022) Development of sintered aggregate derived from POFA and silt for lightweight concrete. J Build Eng. https://doi.org/10.1016/j.jobe.2022.104039
63. Alida A, Mustafa AM, Bakri A, Kamarudin H, Ruzaidi CM, Salleh MAAM, Chin KH (2013) The Effect of Acidic to the Fly Ash Based Geopolymer Artificial Aggregate. Aust J Basic Appl Sci 7:303–307
64. Dong B, Chen C, Wei G, Fang G, Wu K, Wang Y (2022) Fly ash-based artificial aggregates synthesized through alkali-activated cold-bonded pelletization technology. Constr Build Mater. https://doi.org/10.1016/j.conbuildmat.2022.128268
65. Mohamad Ibrahim N, Ismail KN, Che Amat R, Iqbal Mohamad Ghazali M (2018) Properties of cold-bonded lightweight artificial aggregate containing bottom ash with different curing regime. In: E3S Web of Conferences. EDP Sciences
66. Özkan H, Kabay N, Miyan N (2022) Properties of cold-bonded and sintered aggregate using washing aggregate sludge and their incorporation in concrete: a promising material. Sustainability (Switzerland). https://doi.org/10.3390/su14074205
67. Tang P, Xuan D, Poon CS, Tsang DCW (2019) Valorization of concrete slurry waste (CSW) and fine incineration bottom ash (IBA) into cold bonded lightweight aggregates (CBLAs): feasibility and influence of binder types. J Hazard Mater 368:689–697. https://doi.org/10.1016/j.jhazmat.2019.01.112
68. Abbas W, Khalil W, Nasser I (2018) Production of lightweight Geopolymer concrete using artificial local lightweight aggregate. In: MATEC Web of Conferences. EDP Sciences
69. Strokova V, Zhernovsky I, Ogurtsova Y, Maksakov A, Kozhukhova M, Sobolev K (2014) Artificial aggregates based on granulated reactive silica powders. Adv Powder Technol 25:1076–1081. https://doi.org/10.1016/j.apt.2014.02.010

70. Kayali O (2008) Fly ash lightweight aggregates in high performance concrete. Constr Build Mater 22:2393–2399. https://doi.org/10.1016/j.conbuildmat.2007.09.001
71. Wainwright PJ, Cresswell DJF (2001) Synthetic aggregates from combustion ashes using an innovative rotary kiln. woodhouse Lane, Leeds LS29JT, UK
72. Ognjen Rudic, Vilma Ducman, Mirijana Malesev, Vlastimir Radonjanin, Suzana Draganic, Slobodan Supic, Miroslava Radeka (2019) Aggregates obtained by alkali activation of fly ash_ The effect of granulation, pelletization methods and curing regimes _ Enhanced reader. Materials 12(776):1–22
73. Patel J, kumar, Patil H, Patil Y, Vesmawala G, (2018) Production and performance of alkali-activated cold-bonded lightweight aggregate in concrete. J Build Eng 20:616–623. https://doi.org/10.1016/j.jobe.2018.09.012
74. Colangelo F, Messina F, di Palma L, Cioffi R (2017) Recycling of non-metallic automotive shredder residues and coal fly-ash in cold-bonded aggregates for sustainable concrete. Compos B Eng 116:46–52. https://doi.org/10.1016/j.compositesb.2017.02.004
75. Chinnu SN, Minnu SN, Bahurudeen A, Senthilkumar R (2021) Recycling of industrial and agricultural wastes as alternative coarse aggregates: A step towards cleaner production of concrete. Constr Build Mater 287
76. Lau PC, Teo DCL, Mannan MA (2017) Characteristics of lightweight aggregate produced from lime-treated sewage sludge and palm oil fuel ash. Constr Build Mater 152:558–567. https://doi.org/10.1016/j.conbuildmat.2017.07.022
77. Wasserman R, Bentur A (1997) PI1 SOOO8–8846(97)00019–7 Effect of lightweight fly ash aggregate microstructure on the strength of concretes. Elsetier Science Ltd, Israel
78. Hung MF, Hwang CL (2007) Study of fine sediments for making lightweight aggregate. Waste Manage Res 25:449–456. https://doi.org/10.1177/0734242X07077615
79. Li X, He C, Lv Y, Jian S, Liu G, Jiang W, Jiang D (2020) Utilization of municipal sewage sludge and waste glass powder in production of lightweight aggregates. Constr Build Mater. https://doi.org/10.1016/j.conbuildmat.2020.119413
80. Moayeri MS, Ashrafi HR, Beiranvand P (2017) Investigating the physical characteristics of non-structural lightweight aggregate blocks of built with region materials. Buildings. https://doi.org/10.3390/buildings7010002
81. Tang P, Florea MVA, Brouwers HJH (2017) Employing cold bonded pelletization to produce lightweight aggregates from incineration fine bottom ash. J Clean Prod 165:1371–1384. https://doi.org/10.1016/j.jclepro.2017.07.234
82. Güneyisi E, Gesoğlu M, Karaoğlu S, Mermerdaş K (2012) Strength, permeability and shrinkage cracking of silica fume and metakaolin concretes. Constr Build Mater 34:120–130. https://doi.org/10.1016/j.conbuildmat.2012.02.017
83. Satpathy HP, Patel SK, Nayak AN (2019) Development of sustainable lightweight concrete using fly ash cenosphere and sintered fly ash aggregate. Constr Build Mater 202:636–655. https://doi.org/10.1016/j.conbuildmat.2019.01.034
84. Nadesan MS, Dinakar P (2017) Mix design and properties of fly ash waste lightweight aggregates in structural lightweight concrete. Case Studies in Construction Materials 7:336–347. https://doi.org/10.1016/j.cscm.2017.09.005
85. Kou SC, Lee G, Poon CS, Lai WL (2009) Properties of lightweight aggregate concrete prepared with PVC granules derived from scraped PVC pipes. Waste Manage 29:621–628. https://doi.org/10.1016/j.wasman.2008.06.014
86. Gunning PJ, Hills CD, Carey PJ (2009) Production of lightweight aggregate from industrial waste and carbon dioxide. Waste Manage 29:2722–2728. https://doi.org/10.1016/j.wasman.2009.05.021
87. Liu X, Chia KS, Zhang MH (2011) Water absorption, permeability, and resistance to chloride-ion penetration of lightweight aggregate concrete. Constr Build Mater 25:335–343. https://doi.org/10.1016/j.conbuildmat.2010.06.020
88. Punlert S, Laoratanakul P, Kongdee R, Suntako R (2017) Effect of lightweight aggregates prepared from fly ash on lightweight concrete performances. In: Journal of Physics: Conference Series. Institute of Physics Publishing
89. Sahoo S, Selvaraju AK, Suriya Prakash S (2020) Mechanical characterization of structural lightweight aggregate concrete made with sintered fly ash aggregates and synthetic fibres. Cem Concr Compos. https://doi.org/10.1016/j.cemconcomp.2020.103712
90. Li H, Sun D, Wang Z, Huang F, Yi Z, Yang Z, Zhang Y (2020) A review on the pumping behavior of modern concrete. J Adv Concr Technol 18:352–363. https://doi.org/10.3151/jact.18.352
91. Kim YH, Park CB, Choi B, il, Shin TY, Jun Y, Kim JH, (2020) Quantitative measurement of water absorption of coarse lightweight aggregates in freshly-mixed concrete. Int J Concr Struct Mater. https://doi.org/10.1186/s40069-020-00408-x
92. Shin TY, Kim YH, Park CB, Kim JH (2022) Quantitative evaluation on the pumpability of lightweight aggregate concrete by a full-scale pumping test. Case Studies in Construction Materials. https://doi.org/10.1016/j.cscm.2022.e01075
93. Thienel KC, Haller T, Beuntner N (2020) Lightweight concrete-from basics to innovations. Materials 13
94. Haller T, Beuntner N, Gutsch H, Thienel KC (2023) Challenges on pumping infra-lightweight concrete based on highly porous aggregates. Journal of Building Engineering. https://doi.org/10.1016/j.jobe.2022.105761
95. Divyah N, Thenmozhi R, Neelamegam M (2020) Strength properties and durability aspects of sintered-fly-ash lightweight aggregate concrete. Materiali in Tehnologije 54:301–310. https://doi.org/10.17222/MIT.2019.101
96. Dinakar P (2013) Properties of fly-ash lightweight aggregate concretes. Proceedings of Institution of Civil Engineers: Construction Materials 166:133–140. https://doi.org/10.1680/coma.11.00046
97. Chang T-P, Prof A, Shieh M-M (1996) Fracture properties of lightweight concrete
98. Gesoglu M, Özturan T, Güneyisi E (2004) Shrinkage cracking of lightweight concrete made with cold-bonded fly ash aggregates. Cem Concr Res 34:1121–1130. https://doi.org/10.1016/j.cemconres.2003.11.024
99. Chi JM, Huang R, Yang CC, Chang JJ (2002) Effect of aggregate properties on the strength and stiffness of lightweight concrete. Taiwan
100. Tanaka CJ, Mohd. Sam AR, Abdul Shukor Lim N, Awang AZ, Hamzah N, Loo P (2020) Properties of concrete containing blended cement and lightweight artificial aggregate. Malaysian Journal of Civil Engineering 32: https://doi.org/10.11113/mjce.v32n2.629
101. Yap SP, Alengaram UJ, Jumaat MZ (2013) Enhancement of mechanical properties in polypropylene- and nylon-fibre reinforced oil palm shell concrete. Mater Des 49:1034–1041. https://doi.org/10.1016/j.matdes.2013.02.070
102. Liu MYJ, Alengaram UJ, Jumaat MZ, Mo KH (2014) Evaluation of thermal conductivity, mechanical and transport properties of lightweight aggregate foamed geopolymer concrete. Energy Build 72:238–245. https://doi.org/10.1016/j.enbuild.2013.12.029
103. Zhang M H and Gjorv O E 0008–88462990103–5
104. Lo TY, Cui HZ (2004) Effect of porous lightweight aggregate on strength of concrete. Mater Lett 58:916–919. https://doi.org/10.1016/j.matlet.2003.07.036

105. Bogas JA, de Brito J, Figueiredo JM (2015) Mechanical characterization of concrete produced with recycled lightweight expanded clay aggregate concrete. J Clean Prod 89:187–195. https://doi.org/10.1016/j.jclepro.2014.11.015
106. Barnes BD, Diamond S, Dolch WL (1978) Micromorphology of the Interfacial Zone Around Aggregates in Portland Cement Mortar. west Lafayette, Indiana
107. Elsharief A, Cohen MD, Olek J (2005) Influence of lightweight aggregate on the microstructure and durability of mortar. Cem Concr Res 35:1368–1376. https://doi.org/10.1016/j.cemconres.2004.07.011
108. Yliniemi P, Ferreira T, Illikainen, (2017) Development and incorporation of lightweight waste-based geopolymer aggregates in mortar and concrete. Constr Build Mater 131:784–792. https://doi.org/10.1016/j.conbuildmat.2016.11.017
109. Hwang K, Noguchi T, Tomosawa F (2004) Prediction model of compressive strength development of fly-ash concrete. Cem Concr Res 34:2269–2276. https://doi.org/10.1016/j.cemconres.2004.04.009
110. Joseph G, Ramamurthy K (2009) Influence of fly ash on strength and sorption characteristics of cold-bonded fly ash aggregate concrete. Constr Build Mater 23:1862–1870. https://doi.org/10.1016/j.conbuildmat.2008.09.018
111. Lo TY, Cui HZ, Tang WC, Leung WM (2008) The effect of aggregate absorption on pore area at interfacial zone of lightweight concrete. Constr Build Mater 22:623–628. https://doi.org/10.1016/j.conbuildmat.2006.10.011
112. Lau PC, Teo DCL, Mannan MA (2018) Mechanical, durability and microstructure properties of lightweight concrete using aggregate made from lime-treated sewage sludge and palm oil fuel ash. Constr Build Mater 176:24–34. https://doi.org/10.1016/j.conbuildmat.2018.04.179
113. Güneyisi E, Gesoğlu M, Pürsünlü Ö, Mermerdaş K (2013) Durability aspect of concretes composed of cold bonded and sintered fly ash lightweight aggregates. Compos B Eng 53:258–266. https://doi.org/10.1016/j.compositesb.2013.04.070
114. Jiang Y, Ling TC, Shi M (2020) Strength enhancement of artificial aggregate prepared with waste concrete powder and its impact on concrete properties. J Clean Prod. https://doi.org/10.1016/j.jclepro.2020.120515
115. Jacobsen S (2005) Calculating liquid transport into high-performance concrete during wet freeze/thaw. Cem Concr Res 35:213–219. https://doi.org/10.1016/j.cemconres.2004.04.029
116. Zakaria M, Cabrera JG (1996) Performance and durability of concrete made with demolition waste and artificial fly ash-clay aggregates
117. Razak RA, Abdullah MMAB, Hussin K, Ismail KN, Hardjito D, Yahya Z (2016) Performances of Artificial Lightweight Geopolymer Aggregate (ALGA) in OPC concrete. In: Key Engineering Materials. Trans Tech Publications Ltd, pp 29–35
118. Shayan A, Xu A (2006) Performance of glass powder as a pozzolanic material in concrete: a field trial on concrete slabs. Cem Concr Res 36:457–468. https://doi.org/10.1016/j.cemconres.2005.12.012